






Article

Evaluation of Salt Tolerance in Four Self-Rooted Almond Genotypes for Super-High-Density Orchards Under Varying Salinity Levels

Xavier Rius-García ^{1,2} , María Videgain-Marco ^{1,3} , José Casanova-Gascón ^{1,3} , Luis Acuña-Rello ⁴ ,
Raquel Zufiaurre-Galarza ⁵ and Pablo Martín-Ramos ^{4,*} 

¹ Department of Agricultural and Environmental Sciences, Higher Polytechnic School of Huesca, University of Zaragoza, Ctra. Cuarte s/n, 22071 Huesca, Spain; xrius@agromillora.com (X.R.-G.); mvidegain@unizar.es (M.V.-M.); jcasan@unizar.es (J.C.-G.)

² Agromillora Group, Plaça Manel Raventós 3-5, St. Sadurní d'Anoia, 08770 Barcelona, Spain

³ AgriFood Institute of Aragón (IA2, CITA–University of Zaragoza), Ctra. Cuarte s/n, 22071 Huesca, Spain

⁴ Department of Agricultural and Forestry Engineering, ETSIIAA, University of Valladolid, Avda. Madrid 44, 34004 Palencia, Spain; luis.acuna@uva.es

⁵ Department of Analytical Chemistry, Higher Polytechnic School of Huesca, University of Zaragoza. Ctra. Cuarte s/n, 22071 Huesca, Spain; zufi@unizar.es

* Correspondence: pmr@uva.es

Abstract: Increasing soil salinity threatens almond production globally, driving the need for the development of salt-tolerant cultivars. This study investigated the salt tolerance mechanisms of four self-rooted almond genotypes (Vialfas, Guara, Penta, and Avijor) under controlled conditions. Young plants were exposed to four salinity levels (0, 25, 50, and 75 mM NaCl) for 5 months. Growth parameters (trunk diameter, shoot length, fresh and dry weights), physiological responses (chlorophyll fluorescence, gas exchange, Soil–Plant Analysis Development (SPAD)), and mineral content were analyzed. Results show significant genotype-specific responses at the critical salinity threshold of 50 mM NaCl. Under these conditions, Guara and Vialfas maintained higher stem fresh weights (31.4 g and 37 g, respectively), while Avijor showed significant declines. Trunk diameter measurements revealed Vialfas' superior performance (7 mm) compared to Guara and Penta (both around 6 mm), while Avijor exhibited the most significant reduction (5 mm). Chlorophyll fluorescence parameters indicated stress impact, with F_v/F_m values decreasing to 0.84 compared to control values of 0.87. Guara maintained higher K^+/Na^+ ratios in leaves (3.05) compared to Avijor (1.95), while Penta showed better Na^+ exclusion ability with the lowest leaf Na^+ content (0.57%). Cl^- accumulation patterns also differed among genotypes, with Avijor and Vialfas showing higher leaf Cl^- concentrations (0.74% and 0.73%, respectively) compared to Penta (0.44%). Genotype responses across all salinity levels revealed distinct tolerance patterns: Guara maintained growth and physiological functions across treatments, while Penta showed remarkable stability under high salinity. Vialfas exhibited vigor at low salinity but declined sharply at 75 mM NaCl. Avijor demonstrated the highest salt sensitivity. These findings highlight the genetic variability in salt tolerance among almond cultivars and identify potential sources of salt-tolerant traits for breeding programs. The study also provides insights for optimizing genotype selection and management strategies in salt-affected orchards, contributing to more sustainable almond production in challenging environments.

Keywords: *Prunus dulcis*; ion homeostasis; genotype selection; photosynthetic efficiency



Academic Editor: Martin Weih

Received: 2 December 2024

Revised: 20 January 2025

Accepted: 21 January 2025

Published: 24 January 2025

Citation: Rius-García, X.; Videgain-Marco, M.; Casanova-Gascón, J.; Acuña-Rello, L.; Zufiaurre-Galarza, R.; Martín-Ramos, P. Evaluation of Salt Tolerance in Four Self-Rooted Almond Genotypes for Super-High-Density Orchards Under Varying Salinity Levels. *Agriculture* **2025**, *15*, 254. <https://doi.org/10.3390/agriculture15030254>

Copyright: © 2025 by the authors. Licensee MDPI, Basel, Switzerland. This article is an open access article distributed under the terms and conditions of the Creative Commons Attribution (CC BY) license (<https://creativecommons.org/licenses/by/4.0/>).

1. Introduction

The almond tree (*Prunus dulcis* Mill. or *Prunus amygdalus* Batsch) represents a globally significant agricultural crop with deep historical roots in Mediterranean cultivation [1]. Over recent decades, almond cultivation and production have increased steadily, with a growth rate of +196% [2]. The global almond market was valued at USD 7397.62 million in 2022 and is projected to expand at a compound annual growth rate of 4.41%, reaching USD 9583.6 million by 2028 [3]. Rainfed almond cultivation on marginal soils is common in Mediterranean countries, where these orchards have historically held socioeconomic value. In Spain, rainfed almond orchards comprised roughly 67% of the total almond cultivation area in the 2019–2020 agricultural campaign [4]. Traditional low- and medium-density cultivation systems were predominant [5]. These systems feature less than 350 trees per hectare, 6 × 6 m to 8 × 8 m spacing, no mechanization or irrigation, and the use of direct seedlings or vigorous rootstocks [6]. The average productivity of almond groves is significantly higher in the case of irrigated crops: 1600–1800 kg/ha vs. 400 kg/ha for rainfed crops [7].

The development of super-high-density (SHD) irrigated almond orchards since 2010 has revolutionized cultivation practices, building upon three decades of success with SHD olive orchards [8]. These modern systems have demonstrated high agronomic [9,10], economic [11], and environmental sustainability [12]. SHD almond orchards use dwarfing rootstocks and self-rooted ‘Smarttree’ plants developed through in vitro cultivation. Cultivars include Penta, Vialfas, Avijor, and Guara [13]. Trees are planted at 4.0 × 1.5 m spacing (1666 trees per hectare). Early bearing (by the fourth year) and full mechanization increase profitability and sustainability by reducing inputs and costs [5]. As of 2022, over 6500 ha of SHD almond orchards exist globally, with examples in countries such as Spain, Portugal, Italy, the USA, Morocco, Tunisia, Chile, and Turkey [5]. Due to the recent adoption of SHD, research on this system is limited. Studies have focused on cultivar biometrics [14], the impact of spacing on yield and light interception [15,16], light interception in SHD vs. open-center systems [17], and the effects of row orientation and canopy position [8].

The implementation of SHD systems faces critical challenges due to the scarcity of suitable land with full water allocation for almond cultivation (5000–8000 m³/ha). This has led to the adoption of SHD almond orchards based on self-rooted plants in areas with minimal supplemental irrigation (500–700 m³/ha). This concept offers an alternative to both traditional almond orchards and cereal crops. However, poor water quality in many almond-growing areas leads to salt accumulation and stress conditions [18]. Rainfall alone cannot leach accumulated salts, necessitating the use of salt-tolerant cultivars for profitability. Unfortunately, research on the agronomical characteristics of self-rooted almond cultivars remains limited. Only Casanova-Gascón et al. [19] have investigated the performance of these cultivars under various environmental constraints, including limiting soil conditions, revealing some differences in cultivar adaptability. Given the limited research on biotic and abiotic stresses in self-rooted almond plants, this study aims to compare the responses of four self-rooted cultivars (Vialfas, Guara, Penta, and Avijor) to varying saline water treatments. The goal is to understand the morphological, physiological, and biochemical aspects of their salt tolerance. This controlled-environment investigation will evaluate and rank these cultivars based on their response to salt stress.

2. Materials and Methods

2.1. Location and Experimental Design

The experiment was conducted in a polyethylene greenhouse situated at the Escuela Politécnica Superior, Universidad de Zaragoza, in Huesca, Spain (42°07′12.78″ N, 0°26′49.04″ O). In June 2022, uniform 12-month-old rooted trees of four almond cultivars

(Avijor, Guara, Penta, Vialfas) were obtained from Agromillora Iberia nursery (Spain) and transplanted into black plastic pots (15 × 15 × 20 cm, 4.5 L) filled with quartziferous sand (0.05–2.0 mm). During transplantation, the roots were rinsed with deionized water to remove any remaining peat.

The plants were grown for 7 months, and in February 2023, they were pruned to a height of 60 cm. The experiment started on 1st June 2023, when the new main shoot had reached a height of 50 cm, and it continued until 1st November 2023 (5 months). The plants were grown under natural light conditions in the greenhouse, which was maintained at daily temperatures between 18 and 33 °C and day/night relative humidity of 55–85%. An automatic mobile screen was set up at 27 °C to reduce daily temperature, and a ventilation system was automatically engaged to control inside air temperature below 35 °C.

The experimental design was a completely randomized block with a total of 64 trees, with 4 trees per treatment (4 salinity levels) and genotype (4 cultivars) combination.

2.2. Irrigation Management

The nutrient solution used in this experiment was a 1/4-strength Hoagland solution [20], added to the local fresh water with a total electrical conductivity (EC) of 0.8 dS m⁻¹. The four genotypes were subjected to four salt levels (0, 25, 50, and 75 mM NaCl) for 5 months. Salt concentrations were increased by 25 mM NaCl per week until the desired concentrations had been reached (1 June).

Weather conditions determined the frequency and duration of irrigation, with 4 min sessions occurring one to three times daily. Each pot had two drippers with a flow rate of 1.3 L h⁻¹ (Click Tip HD, Naandanjain, Jalgaon, India). Salinity solutions were injected by a MixRite E-300 volumetric pump (Tefen Flow and Dosing Technologies Ltd., Kibbutz Farod, Israel), and irrigation was controlled by an Agronic 5500 irrigation controller (Sistemas Electrònics PROGRÉS, Barcelona, Spain).

The EC and sodium absorption ratio (SAR) levels for the irrigation waters were 0.8, 3.0, 6.0, and 9.0 dS m⁻¹ and 2, 30, 60, and 90, respectively, with pH values ranging between 7.2 and 7.4. During the experiment, the drainage water from each treatment was collected and analyzed for leached solutes. Weekly electrical conductivity measurements in the leaching solution were carried out using a Hanna Instruments-HI 9033 conductivity meter (Woonsocket, RI, USA). The values obtained were 0.8, 3.2, 6.1, and 9.2 dS m⁻¹, corresponding to the concentrations of 0, 25, 50, and 75 mM NaCl, respectively. This confirmed that maintaining a leaching fraction of 20–30% during irrigation ensures a consistent level of salinity in the pots throughout the experiment [21].

2.3. Plant Material Analysis

Every 15 days, shoot length, trunk diameter at 10 cm (using a digital ABS caliper, Hoffman Group, Munich, Germany), and visual damage of four plants per treatment were measured. Salt-induced leaf necrosis was assessed visually on four plants per treatment using a scale from 0 to 5, based on the percentage of total leaf area affected (0: no symptoms; 1: 20%; 2: 40%; 3: 60%; 4: 80%; 5: more than 80% of the plant canopy). Values for each treatment represent the average of four plant replicates.

At the end of the experiment, four plants of each treatment for each cultivar were removed from the substrate and partitioned into various parts (roots, wood, new shoots, and leaves). Aerial plant parts were washed with distilled water, and roots were washed with deionized water. The fresh masses of all plant parts were recorded, and they were then dried at 70 °C for 24 h to determine their dry weights.

The dried plant materials were ground into particles smaller than 2 mm using an electrical grain grinder (CGoldenwall model HC400, Wuxi, China). These particles were then analyzed using both wet chemistry and a Niton XL3t GOLDD+ portable X-ray fluorescence (pXRF) spectrometer (Thermo Scientific, Waltham, MA, USA). The <2 mm particle size was chosen to simulate the physical conditions of processed soil samples that can be measured by a pXRF probe, following the findings of Sapkota et al. [22], Antonangelo and Zhang [23], and Towett et al. [24]. The pXRF was used to quickly and efficiently measure the concentrations of Ca^{2+} , K^+ , and Cl^- without any pretreatment, using the 'Soil mode' for Ca^{2+} and K^+ , and the 'Mining mode' for Cl^- [25,26]. The pXRF measurements for cations were calibrated using atomic absorption spectrometry as a reference method to ensure the accuracy of the elemental analysis. For Cl^- calibration, samples were analyzed by ionic chromatography at an external laboratory (Eurofins Scientific, Sidamon, Lleida, Spain).

For the determination of sodium content, the dried and ground plant materials were digested using the nitric acid digestion method. Approximately 0.5 g of each sample was predigested for 1 h with 10 mL of trace metal-grade HNO_3 . The digests were then heated to 115 °C for 2 h and diluted with deionized water to 50 mL [27]. Sodium content in the digested samples was determined by atomic absorption spectrometry (SpectrAA 10, Varian, CA, USA), as described by Kalra [28]. All values reported are the averages of four repeated measurements.

2.4. Physiological Parameters

2.4.1. Leaf Chlorophyll (SPAD)

Every two weeks, total chlorophyll content was determined using a portable SPAD-502Plus (Konica Minolta, Osaka, Japan) chlorophyll meter, allowing rapid, non-destructive measurements. SPAD values were obtained from fully expanded functional leaves, with the meter shielded from direct sunlight by the operator during each measurement. Fifteen leaves were randomly selected from each cultivar and treatment, and their values were averaged to obtain a single SPAD value.

2.4.2. Chlorophyll Fluorescence

Chlorophyll fluorescence parameters were recorded every two weeks using a portable Handy PEA fluorimeter (Hansatech Instruments Ltd., Norfolk, UK). Parameters including initial (F_0), maximum (F_m), variable ($F_v = F_m - F_0$) fluorescence, and maximum quantum yield of photosystem II (PSII) (F_v/F_m) in dark-adapted leaves, among others, were recorded. The parameters obtained from the fluorimeter were divided into 3 groups: overall efficiency of photosystem II, energy and electron transport, and energy dissipation and damage [29–31].

2.4.3. Stomatal Conductance

Every two weeks, stomatal conductance (g_s , $\text{mmol H}_2\text{O m}^{-2} \text{s}^{-1}$) was measured using a portable porometer (SC-1 Meter Group, Washington, DC, USA). Measurements were made on two well-exposed and fully expanded leaves from the median part of the shoot from four plants per treatment and cultivar, between 9:00 am and 11:00 am.

2.5. Statistical Analysis

All statistical analyses were performed using R software (v. 4.4.1:2024) [32]. A complete 3-factor factorial design was established (genotype, treatment, and organ) with 4 levels each and 4 repetitions, having a total of $4^3 \times 4 = 256$ trials. The analysis of the samples from each trial allowed obtaining the values of the target variables: Ca^{2+} , Na^+ , K^+ , Cl^- , fresh weight, and dry weight. Along with these variables, the behavior of the most important

relationships between them was analyzed: $\text{Ca}^{2+}/\text{Na}^{+}$ and $\text{K}^{+}/\text{Na}^{+}$. The normality of the data was checked for all populations using the Kolmogorov–Smirnov normality test with Lilliefors correction [33] or the Shapiro–Wilk test [34], according to the amount of data in the groups, and the Q–Q normal probability plot. This test was virtually always unfulfilled. The requirement of homoscedasticity was contrasted by the Levene test [35], being defaulted in many cases, so the usual comparative analysis that provides linear statistics, ANOVA, cannot be used. To solve this impediment, two statistical techniques were used: the Kruskal–Wallis test [36], when the distribution was not normal but the groups were homoscedastic; Welch’s heteroscedastic F test with trimmed means and Winsorized variances, when neither normality nor homoscedasticity could be assumed. This latter robust procedure tests the equality of means by substituting trimmed means and Winsorized variances for the usual means and variances [37,38]. Also, bootstrap methods were used to establish robust confidence intervals for location [39] and robust homogenous groups.

The response models, natural cubic spline models [40–42], were used, analyzing their performance for each target variable (trunk diameter, shoot length, SPAD, and stomatal conductance), which was evaluated employing residual analysis, the correlation coefficient (R^2 value) [43], the Akaike information criterion (AIC) [44], and the Bayesian information criterion (BIC) [45,46]. These values, together with the likelihood-ratio test and Wald’s test, make it possible to establish the model’s goodness-of-fit.

3. Results

3.1. Growth Parameters Under Salinity Stress

3.1.1. Fresh and Dry Weight

Figure S1 illustrates the pattern of fresh-weight distribution across treatments and organs: stems > wood > roots > leaves. Salinity effects varied by organ, with leaves showing the highest sensitivity, particularly in Avijor and Penta (Figure S2). Roots exhibited diverse responses, while wood weights remained relatively stable. Detailed statistical comparisons, including significance groupings, are provided in the Supporting Information (“Rob Groups” column in the accompanying tables).

Concerning the dose effect on fresh weight, at 0 mM NaCl, all genotypes showed strong growth, with Vialfas performing best (Figure S3). At 25 mM NaCl, Vialfas and Guara maintained or increased stem fresh weight, while Avijor and Penta showed significant decreases (Figure S2). At 50 mM NaCl, Guara and Vialfas retained relatively high stem fresh weights, while Avijor showed further declines. At 75 mM NaCl, Avijor exhibited a partial recovery in root, wood, and stem weights compared to 50 mM NaCl.

Dry weight showed a similar pattern of distribution across organs, with stems having the highest values (11.67–19.32 g), followed by wood and roots (10.12–11.54 g and 8.88–10.71 g, respectively), and leaves (4.33–5.82 g) across all treatments (Figure S4). The organ response to salinity varied among genotypes, with leaves showing the highest sensitivity, particularly in Avijor (Figure S5). When examining overall genotype responses to salinity, Vialfas and Guara demonstrated higher tolerance compared to other genotypes (Figure S6). Vialfas showed the highest total dry weight under control conditions (16.56 g) and maintained high values under moderate salinity at 25 mM NaCl (15.79 g), though decreasing at higher salinity levels (11.65 g at 50 mM and 9.00 g at 75 mM NaCl). Guara maintained stable dry weight values across treatments (9.84–10.14 g, Figure S6). Avijor exhibited significant sensitivity to moderate salinity, with total dry weight decreasing from 9.76 g in control to 4.94 g at 25 mM NaCl, though showing recovery at 75 mM NaCl (10.04 g). Penta displayed intermediate sensitivity, declining from 11.23 g in control to 7.97 g at the highest salinity (Figure S6).

3.1.2. Trunk Diameter

Table S1 presents spline data illustrating the differences in trunk diameter among genotypes and treatments. Under control conditions (Figure 1a), Vialfas demonstrated the most robust growth (8 mm final diameter), followed by Guara (7.5 mm), while Avijor and Penta exhibited similar growth patterns (7 mm and 6.5 mm, respectively). At 25 mM NaCl (Figure 1b), Vialfas maintained superior growth, but Guara declined to 6 mm, and Avijor and Penta showed slight reductions. At 50 mM NaCl (Figure 1c), trunk diameter growth decreased across all genotypes, with Vialfas outperforming (7 mm), Guara and Penta showing similar growth (6 mm), and Avijor exhibiting the most significant reduction (5 mm). At 75 mM NaCl (Figure 1d), Guara showed the best performance (6.5 mm); Penta and Avijor displayed similar growth patterns (6 mm); while Vialfas, which had excelled at lower salinity, showed the poorest performance (5.5 mm).

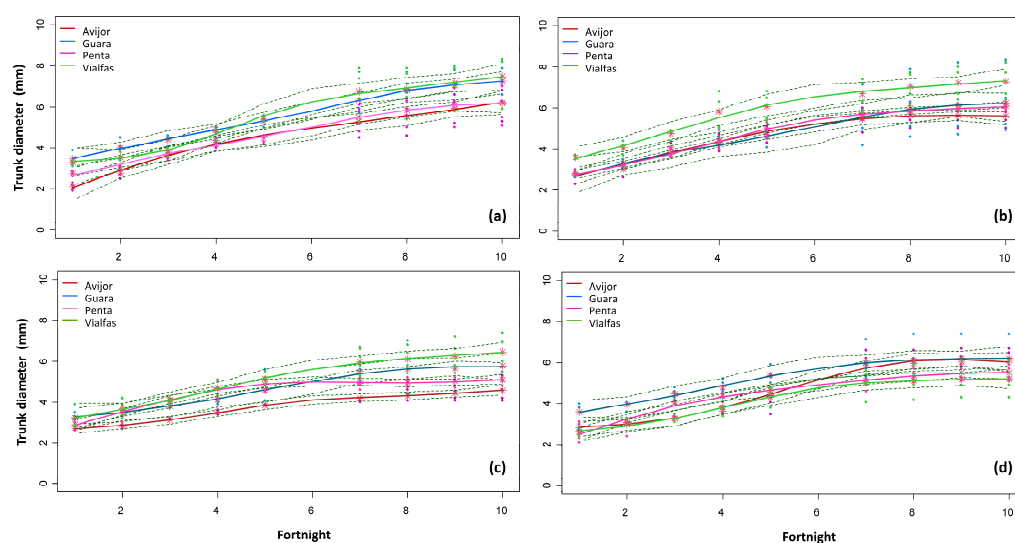


Figure 1. Trunk diameter evolution for the four *Prunus* genotypes as a function of salinity: (a) control, (b) 25 mM NaCl, (c) 50 mM NaCl, and (d) 75 mM NaCl. For each genotype, the central line represents the fitted spline curve, while dotted lines above and below represent the 95% confidence intervals.

3.1.3. Shoot Length

Spline data of genotype and treatment effects on shoot length are presented in Table S2. Under control conditions (Figure 2a), Vialfas demonstrated the most vigorous growth (final height of 160 cm), followed by Avijor and Guara (140 cm and 135 cm, respectively), and Penta (120 cm). At 25 mM NaCl (Figure 2b), Vialfas maintained superior growth, with Avijor nearly matching Vialfas by the end of the period, and Guara and Penta showing slower growth rates. At 50 mM NaCl (Figure 2c), growth was significantly reduced in all genotypes, with diminished genotypic differences under higher stress. At 75 mM NaCl (Figure 2d), growth was severely stunted for all genotypes, with Penta performing relatively better under extreme stress and Avijor showing the poorest performance.

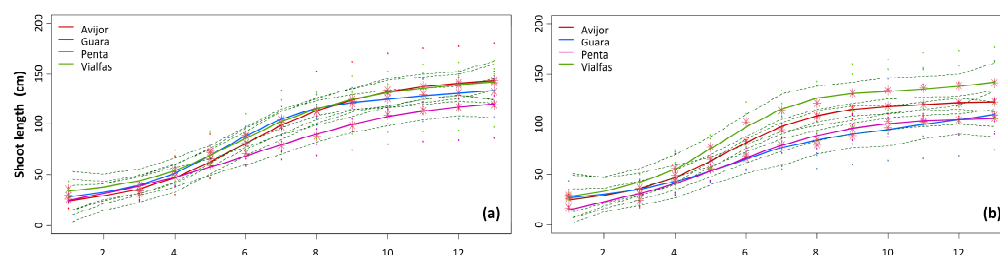


Figure 2. Cont.

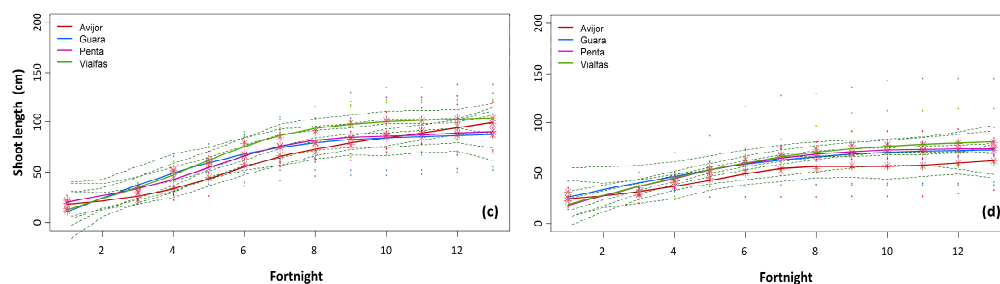


Figure 2. Shoot length evolution for the four *Prunus* genotypes as a function of salinity: (a) control, (b) 25 mM NaCl, (c) 50 mM NaCl, and (d) 75 mM NaCl. For each genotype, the central line represents the fitted spline curve, while dotted lines above and below represent the 95% confidence intervals.

3.2. Physiological Responses to Salinity Stress

3.2.1. Chlorophyll Fluorescence Parameters

Increasing salinity negatively impacted photosynthetic parameters ($\phi(Po)$, PI_{abs} , PI_{Inst} , and F_v/F_m) and electron transport parameters (REo/RC and $\psi(Eo)$) across all genotypes (Figure 3a,b). Penta and Avijor maintained relatively stable photosynthetic yield and electron transport, while Guara and Vialfas showed significant reductions, with Guara experiencing a near collapse of electron flow at 75 mM NaCl. Energy dissipation (DIo/RC and DIo/CSo ; Figure 3c) increased with salinity, with tolerant genotypes showing more controlled increases.

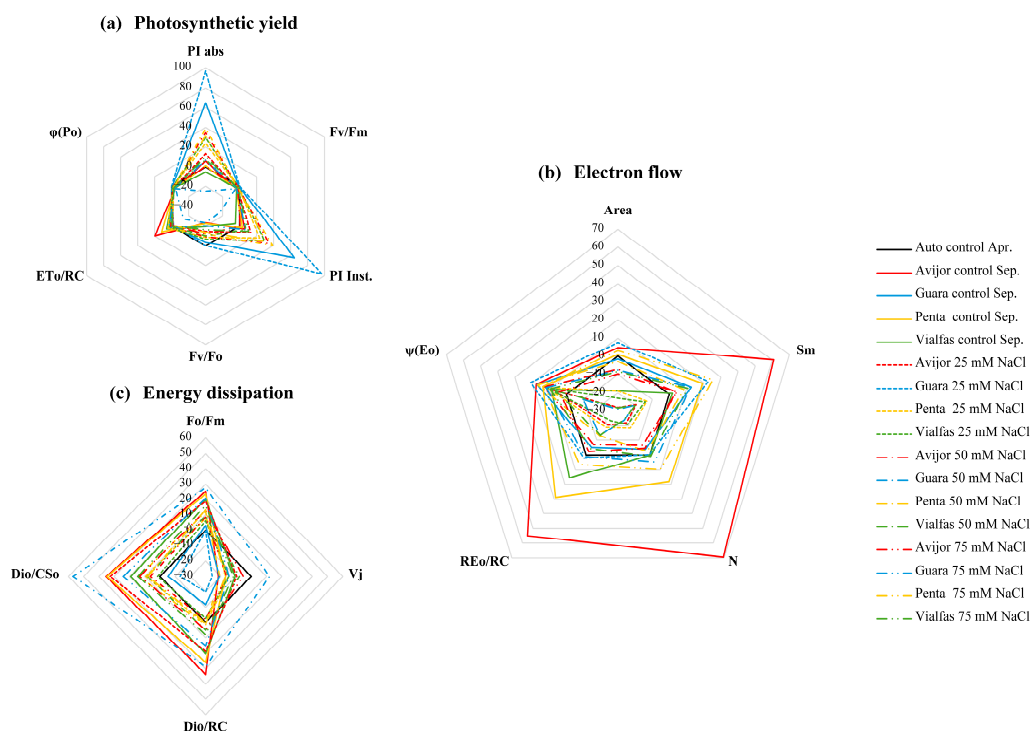


Figure 3. (a) Photosynthetic performance, (b) electron flow, (c) and energy dissipation for the different *Prunus* genotypes as a function of salinity at the end of the experiment. ‘Auto control Apr.’ represents the average of all genotypes in April. Area represents the area above the fluorescence induction curve between the minimum fluorescence (F_0) and the maximum fluorescence (F_m) and is related to the pool size of electron acceptors in the photosynthetic electron transport chain. F_v/F_m is the maximum quantum efficiency of photosystem II (PSII) when all reaction centers are open. V_j represents the relative variable fluorescence at the J-step of the OJIP fluorescence transient and provides information about the reduction state of the primary quinone electron acceptor (QA). Sm is the normalized total complementary area above the OJIP transient and is related to the energy needed to close all PSII reaction centers. N represents the turnover number of QA, which is the number of times QA is reduced

and oxidized during the measurement. DIo/RC is the energy dissipated in the form of heat and fluorescence per reaction center. ETo/RC represents the electron transport rate per reaction center. REo/RC is the rate of electron transport beyond QA per reaction center. $\phi(Po)$ is the maximum quantum yield of primary photochemistry. $\psi(Eo)$ represents the efficiency with which a trapped exciton can move an electron into the electron transport chain beyond QA. DIo/CSo is the energy dissipated in the form of heat and fluorescence per cross-section. PI_{abs} is the performance index on an absorption basis, which combines several fluorescence parameters to provide an overall measure of the performance of PSII.

Critical measurements of PSII efficiency showed that both seasonal changes and saline stress negatively affected PSII performance (Table S3 and Figure S7), reflected in reductions in F_v/F_m and PI_{abs} . At 75 mM NaCl, photosynthetic yield collapsed, though Penta and Avijor showed some recovery at 50 and 75 mM NaCl (Figure 3a,b). Electron transfer capacity decreased under stress, indicated by reductions in REo/RC and $\psi(Eo)$ (Figure S8). At 25 and 50 mM NaCl, adjustments in Area and Sm parameters suggested compensation attempts, but at 75 mM NaCl, compensation capacity was overwhelmed. Energy dissipation increased with stress, as evidenced by rising DIo/RC and DIo/CSo levels (Figure S9), with the V_j parameter showing QA accumulation at 75 mM NaCl.

3.2.2. Gas Exchange

Statistical data on stomatal conductance across treatments and genotypes are summarized in Table S4. Under control conditions, all genotypes exhibited similar patterns (Figure 4a–d), with Penta reaching the highest peak conductance around the fourth fortnight and Vialfas maintaining the most stable conductance throughout. At 25 mM NaCl, Penta maintained the highest conductance, especially early on, while Vialfas showed a marked decrease. At 50 mM NaCl, conductance decreased for all genotypes, with Avijor showing the lowest conductance throughout. At 75 mM NaCl, Penta showed the most significant reduction, while Vialfas maintained the most stable pattern, albeit at low conductance levels.

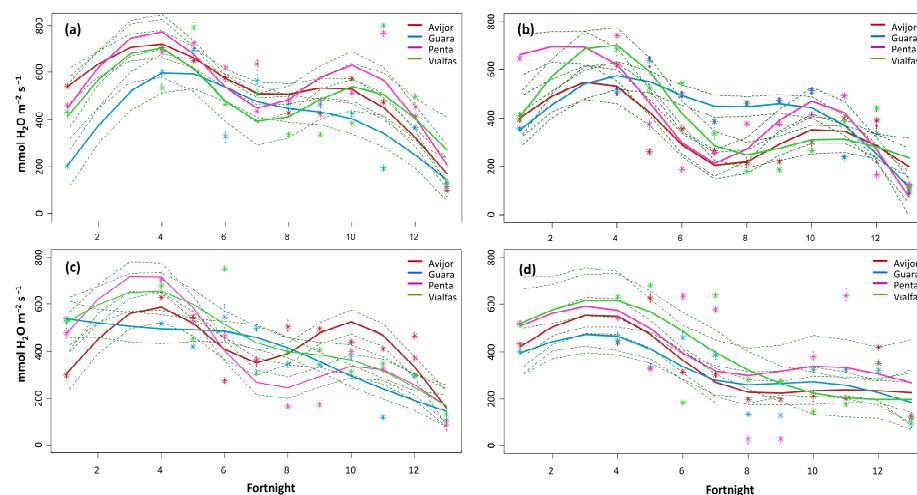


Figure 4. Stomatal conductance (gs , $\text{mmol H}_2\text{O m}^{-2} \text{s}^{-1}$) evolution for the four *Prunus* genotypes as a function of salinity: (a) control, (b) 25 mM NaCl, (c) 50 mM NaCl, and (d) 75 mM NaCl. For each genotype, the central line represents the fitted spline curve, while dotted lines above and below represent the 95% confidence intervals.

3.2.3. Chlorophyll Content Analysis by Soil–Plant Analysis Development (SPAD)

Statistical data on SPAD across treatments and genotypes are summarized in Table S5. Under control conditions, all genotypes showed increasing SPAD values over time (Figure 5a–d), with Guara demonstrating the highest values. At 25 mM NaCl, Guara

maintained high SPAD values with strong increases, while Penta displayed relatively stable values. At 50 mM NaCl, Guara showed high variability, with a sharp decline around the sixth fortnight followed by recovery, while Avijor demonstrated steady increases. At 75 mM NaCl, Guara showed a strong increase in SPAD values over time, while Penta maintained relatively low but stable values.

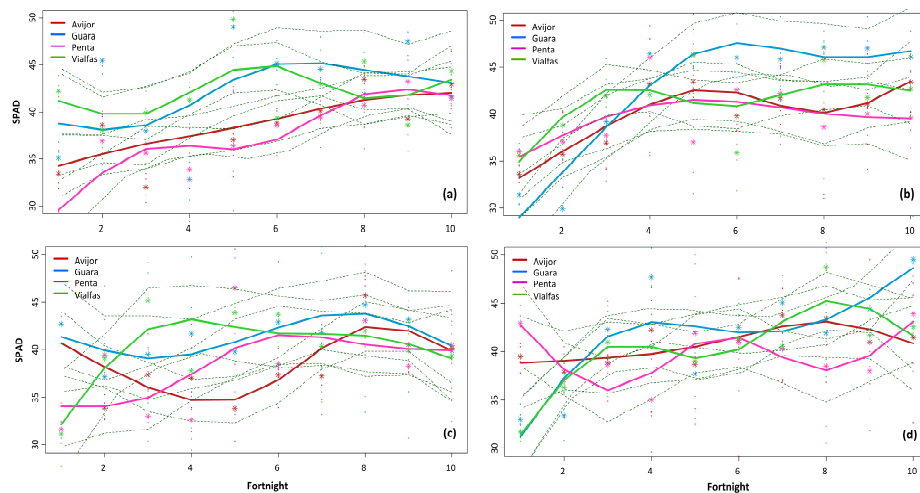


Figure 5. SPAD evolution for the four *Prunus* genotypes as a function of salinity: (a) control, (b) 25 mM NaCl, (c) 50 mM NaCl, and (d) 75 mM NaCl. For each genotype, the central line represents the fitted spline curve, while dotted lines above and below represent the 95% confidence intervals.

3.3. Visual Salinity Stress Symptoms

All genotypes exhibited robust growth under non-saline conditions, characterized by abundant dark green leaves distributed evenly along the stem, well-developed root systems, and healthy overall plant structure (Figure 6). At 25 mM NaCl, stress symptoms emerged through slight reductions in leaf density, size, and root system volume. At 50 mM NaCl, moderate-to-severe stress symptoms appeared, including a noticeable reduction in leaf number with chlorosis and necrosis at margins, thinner and shorter stems, and reduced root system volume and branching. At 75 mM NaCl, all genotypes showed severe stress symptoms, with an important reduction in leaf number and extensive chlorosis and necrosis in the remaining leaves, noticeably thinner and shorter stems, and severely impacted root systems showing minimal development and branching.

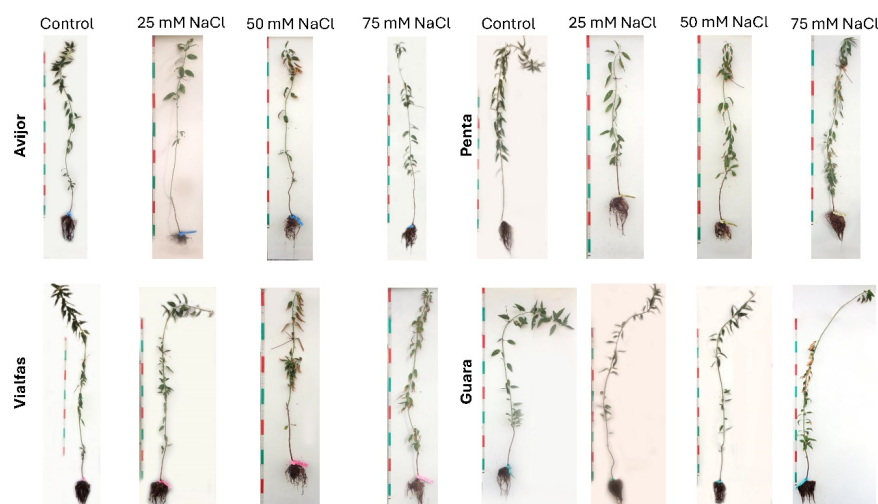


Figure 6. Visual aspect of the four genotypes subjected to the various salinity treatments at the end of the experiment. Only one replicate per treatment is shown.

Regarding leaf damage, as shown on the 0–5 scale in Figure 7a, Avijor and Guara demonstrated remarkable resilience at 25 mM NaCl (Figure 7c), showing no measurable damage, while Penta and Vialfas exhibited slight susceptibility, with integrated damage over time (represented by the area under the damage progression curves) values of 5.49 and 3.30, respectively. At 50 mM NaCl (Figure 7d), Vialfas showed the highest accumulated damage (21.98), followed by Guara (12.09) and Penta (8.79), while Avijor maintained relatively low damage levels (3.30). Under 75 mM NaCl (Figure 7e), Penta exhibited the highest integrated damage (30.77), followed by Vialfas (29.67), while Avijor (20.88) and Guara (19.78) showed comparatively better resilience.

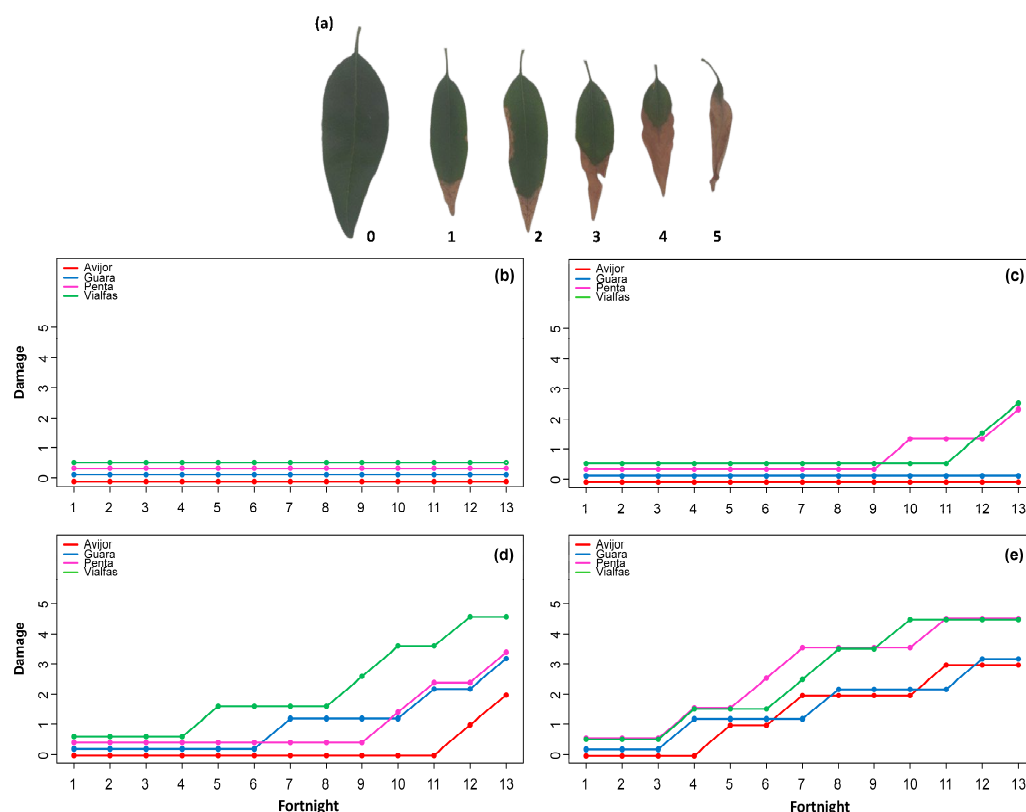


Figure 7. (a) Leaf damage level scale, (b–e) leaf damage evolution for each of the four *Prunus* genotypes as a function of salinity: (b) control, (c) 25 mM NaCl, (d) 50 mM NaCl, and (e) 75 mM NaCl. Values on the y-axis represent instantaneous damage levels on the 0–5 scale, while integrated values discussed in the text represent the area under these damage progression curves over time. For better visualization, damage progression curves have been vertically offset where overlapping occurs, while maintaining their relative patterns and actual damage scale values.

3.4. Changes in Mineral Content Under Salinity Stress

Given the data structure (Table S6), logarithmic transformations were applied to the dependent variables due to deviation from normality assumptions. This approach facilitated the construction of general factorial models for ANOVA analyses (Table S7). The model structure was defined as:

$$\log(\text{Dependent variable}) \sim \text{fact.A}(\text{Genotype}) \times \text{fact.B}(\text{Treatment}) \times \text{fact.C}(\text{Organ})$$

All three factors proved significant across all models. Robust comparison methods were employed to address heteroscedasticity and non-normality issues. The untransformed variables were used for these comparisons (Table S8), as deemed more appropriate given the data characteristics (Figures 8 and 9).

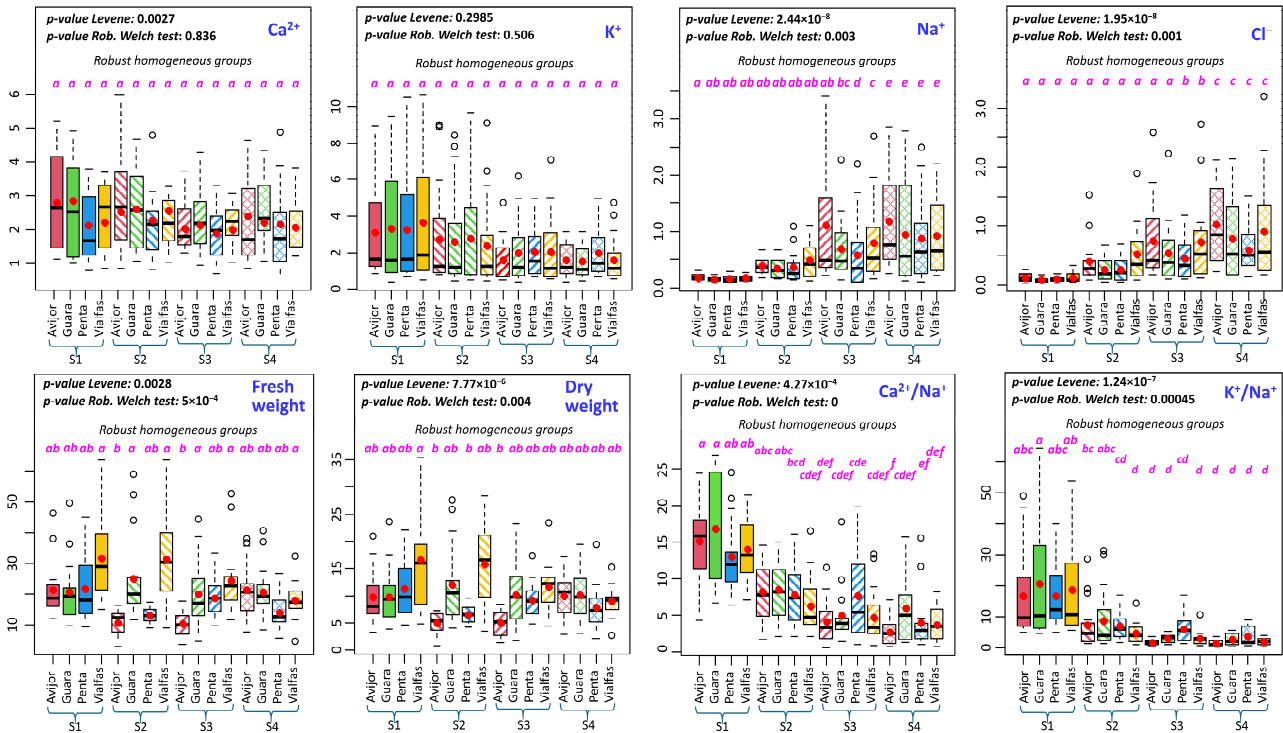


Figure 8. Box-plot of cations and anions for the genotype \times salinity treatment interactions. S1, S2, S3, and S4 stand for control, 25, 50, and 75 mM NaCl, respectively. Different letters indicate significantly different groups based on robust homogeneous groups statistical analysis ($p < 0.05$).

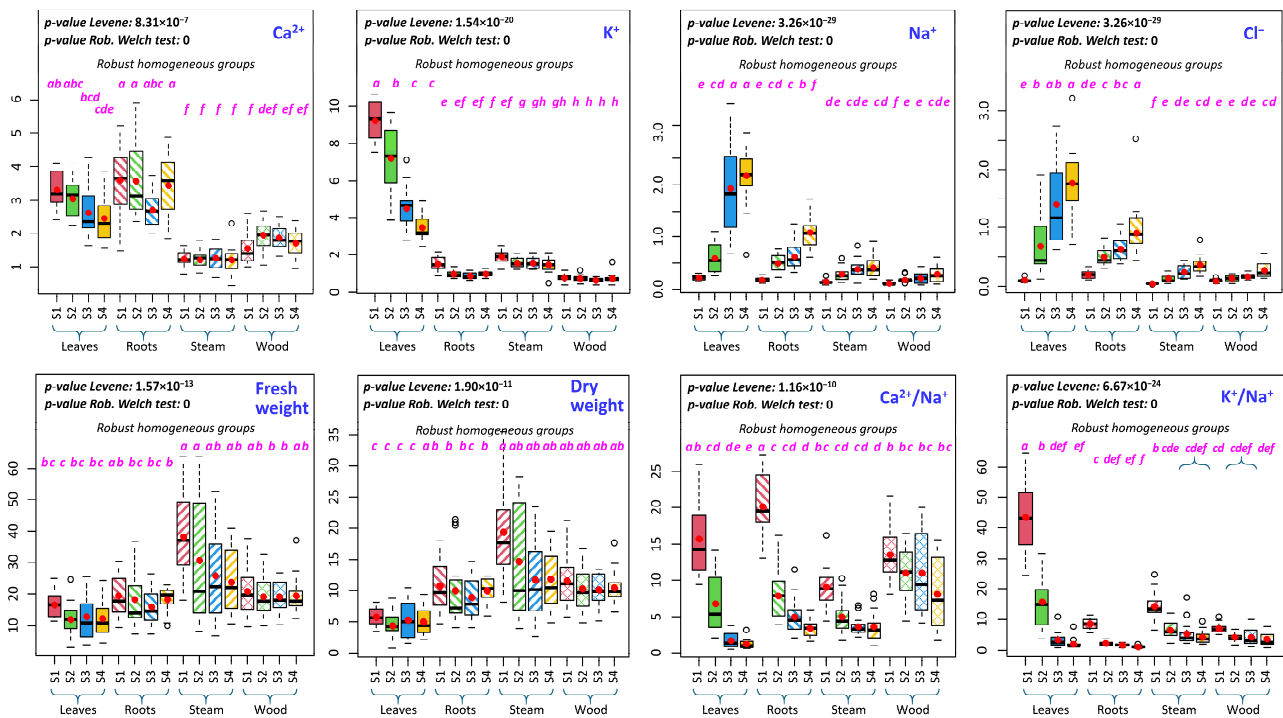


Figure 9. Box-plot of cations and anions for the organ \times salinity treatment interactions. S1, S2, S3, and S4 stand for control, 25, 50, and 75 mM NaCl, respectively. Different letters indicate significantly different groups based on robust homogeneous groups statistical analysis ($p < 0.05$).

The statistical significance of differences between treatments, genotypes, and organs for all mineral analyses can be found in the Supporting Information (Figures S10–S27, “Rob Groups” column in the accompanying tables).

3.4.1. Calcium Content and Distribution

When examining organ-specific responses (Figure S10), roots consistently showed the highest Ca^{2+} content across genotypes, with the highest content in control (3.59%) and 25 mM NaCl (3.58%) treatments, decreasing at 50 mM NaCl (2.69%) and increasing at 75 mM NaCl (3.45%). Leaves showed the second-highest Ca^{2+} content, gradually decreasing with increasing salinity. Wood demonstrated moderate Ca^{2+} content with a non-linear response to salinity, increasing from control (1.53%) to 25 mM NaCl (1.93%), then gradually decreasing. Stems showed the lowest Ca^{2+} content (1.20–1.26%).

Regarding genotype-specific responses (Figures S11 and S12), Avijor exhibited the highest mean root Ca^{2+} content (4.12%, 27–39% higher than other genotypes), though showing a variable response to salinity. Guara maintained consistently high Ca^{2+} levels across salinity treatments, showing the highest mean leaf Ca^{2+} content (3.54%) and stem content (1.37%). Penta displayed lower Ca^{2+} levels across all organs and treatments. Vialfas showed moderate Ca^{2+} levels with less variability, having the highest wood Ca^{2+} content (1.92%).

3.4.2. Potassium Accumulation Patterns

Potassium distribution also varied across plant organs (Figure S13), with leaves showing the highest K^+ content (5.52–6.39%), followed by stems (1.48–1.82%), roots (1.01–1.19%), and wood (0.66–0.78%). Leaf K^+ content decreased from 9.23% in the control to 3.47% at 75 mM NaCl. Stems showed a moderate but consistent decrease (24% reduction), while roots and wood exhibited complex, non-linear responses.

Genotype-specific responses (Figures S14 and S15) showed Avijor's consistent decrease in mean K^+ content from 3.12% in the control to 1.57% at 75 mM NaCl. Penta maintained slightly higher K^+ levels (2.78% at 25 mM NaCl to 1.98% at 75 mM NaCl). Vialfas demonstrated the highest control K^+ content (3.68%) but experienced significant decreases with increasing salinity. Guara reached the lowest K^+ content (1.51%) at 75 mM NaCl.

3.4.3. Chloride Accumulation and Distribution

Organ-specific patterns (Figure S16) showed leaves with the highest Cl^- content (0.64–1.24%), followed by roots (0.45–0.66%), stems (0.14–0.28%), and wood (0.13–0.19%). Control Cl^- content was low (0.04–0.19%), increasing significantly at 25 mM NaCl, particularly in leaves and roots. At 50 mM NaCl, Cl^- accumulation intensified, with leaf tissue exhibiting the most pronounced increase in concentration. At 75 mM NaCl, Cl^- accumulation reached its peak: leaf Cl^- content increased 18-fold from control to 75 mM NaCl, root content increased 4.75-fold, stems 7.9-fold, and wood 2.9-fold.

Concerning genotype influence, Avijor and Vialfas showed steeper Cl^- content increases from control to 75 mM NaCl, while Penta showed a more gradual increase (Figures S17 and S18). At 50 mM NaCl, Avijor and Guara grouped separately from Penta and Vialfas in statistical analyses. At 75 mM NaCl, Vialfas and Avijor accumulated more leaf Cl^- (1.25 and 1.23%, respectively), compared to Penta and Guara. Vialfas showed the highest root Cl^- content (0.67%), while Penta showed consistently lower Cl^- accumulation.

3.4.4. Sodium Content and Distribution

Sodium distribution varied across plant organs (Figure S19), with leaves showing the highest Na^+ content (1.05–1.59%), followed by roots (0.45–0.73%), stems (0.23–0.42%), and wood (0.17–0.27%). Control Na^+ content was low (0.11–0.22%), increasing moderately at 25 mM NaCl and significantly at 50 mM NaCl (1.92% in leaves). Leaves showed a 9.7-fold increase from control to 75 mM NaCl, roots 5.9-fold, stems 2.9-fold, and wood 2.5-fold.

About the influence of the genotype (Figures S20 and S21), Avijor consistently accumulated the highest Na^+ levels, reaching 1.10% at 50 mM NaCl and 1.19% at 75 mM

NaCl. Penta demonstrated superior Na⁺ exclusion, particularly at 50 mM NaCl. Guara and Vialfas exhibited intermediate Na⁺ accumulation. At 50 mM NaCl, genotypes were spread across different statistical groups, while at 75 mM NaCl, all genotypes showed significant differences versus lower salinity treatments but not versus each other.

3.4.5. Potassium/Sodium Ratio Analysis

Organ-specific patterns revealed consistent trends across genotypes (Figure S22). Leaves showed the highest K⁺/Na⁺ ratios (13.01–20.81), but they dramatically decreased from 43.44 in control to 1.93 under 75 mM NaCl. Roots exhibited moderate K⁺/Na⁺ ratios (2.88–4.24), declining from 8.54 in control to 1.02 under 75 mM NaCl. Wood and stem tissues showed intermediate and relatively stable K⁺/Na⁺ ratios across treatments, decreasing from 6.99 in control to 3.48 under 75 mM NaCl and from 14.28 to 4.17, respectively.

In relation to the genotype-specific responses (Figures S23 and S24), Guara exhibited the highest mean K⁺/Na⁺ ratio (20.82) in control, followed by Vialfas (18.98). Penta had the highest K⁺/Na⁺ ratios in stems (10.43) and wood (6.21). Under 75 mM NaCl, Penta maintained relatively higher K⁺/Na⁺ ratios, particularly in roots and stems, while Avijor showed the lowest K⁺/Na⁺ ratio (1.65).

3.4.6. Calcium/Sodium Ratio Analysis

Roots maintained higher Ca²⁺/Na⁺ ratios (6.75–10.17) compared to other organs across all genotypes (Figure S25). Wood tissues also exhibited relatively high Ca²⁺/Na⁺ ratios, particularly in Penta (12.29) and Guara (11.28). Leaves showed the most variable Ca²⁺/Na⁺ ratios among genotypes (4.42–9.45), while stems generally showed lower Ca²⁺/Na⁺ ratios (4.46–5.85).

Concerning the impact of genotype, in control conditions, Ca²⁺/Na⁺ ratios ranged from 12.94 to 16.67 (Figures S26 and S27). Guara maintained relatively higher Ca²⁺/Na⁺ ratios across all treatments, while Avijor showed the most dramatic decline at 50 and 75 mM NaCl. Penta and Vialfas displayed intermediate responses, with Penta showing slightly better maintenance of Ca²⁺/Na⁺ ratios at higher salinities. At 75 mM NaCl, the Ca²⁺/Na⁺ ratios converged to lower values across all genotypes (2.69–5.99).

4. Discussion

4.1. Growth Parameters Under Salinity Stress

4.1.1. Fresh and Dry Weight

Our results corroborate the findings by Zrig et al. [47] and Sandhu et al. [48], who reported significant variability in salt tolerance among almond rootstocks (GFF 677, GN15, *P. dulcis*, and 14 other commercial almond rootstock genotypes—including peach hybrids and peach-almond hybrids). Vialfas exhibited superior vigor, especially under control conditions, suggesting inherent traits conducive to robust growth and potential salt tolerance. In turn, Guara displayed the highest resilience across salinity treatments, maintaining growth under stress conditions.

Guara's ability to sustain high fresh and dry weights under salinity stress—and even increase stem weight at 25 mM NaCl—suggests potential salt tolerance mechanisms. This stress-induced growth response could be attributed to osmotic adjustment or efficient ion compartmentalization, as Munns and Tester [49] suggest in their review of salinity tolerance mechanisms. In contrast, the sensitivity of Avijor, which experienced sharp weight declines at moderate salinity levels, highlights the genetic basis of salt tolerance in *Prunus*. Similar genetic variability has been noted by Toro et al. [50] in their study on *Prunus* rootstocks with genetic backgrounds from the subgenera *Prunus*, *Cerasus*, and *Amygdalus*.

Organ-specific responses provide additional insights into salt stress adaptation strategies in *Prunus*. The prioritization of stem and wood growth over leaf production under salt stress aligns with observations by Zrig et al. [47] in almond rootstocks. This allocation pattern may serve as an adaptive strategy to maintain structural integrity under stress conditions, as proposed by Tattini et al. [51] in their research on olive trees.

The varied root responses, particularly the increased root growth observed in Vialfas under moderate salinity, suggest adaptive mechanisms to enhance resource acquisition under stress. Similar stimulation of root growth under moderate salinity has been reported in other woody species [52]. This response could be crucial for salt tolerance, given that roots play a vital role in ion exclusion and water uptake in saline environments [53]. The non-linear responses to increasing salinity, especially the partial recovery of some genotypes at 75 mM NaCl, may indicate the activation of stress response mechanisms at high salinity levels. This phenomenon, observed in other plant species, could involve the induction of antioxidant systems or osmolyte accumulation [54].

4.1.2. Trunk Diameter

The superior salt tolerance exhibited by Vialfas at 25 mM and 50 mM NaCl, as evidenced by its sustained trunk diameter growth, corroborates previous research on salt-resistant *Prunus* cultivars. For instance, Zrig et al. [55] reported similar variability in salt tolerance among different *Prunus* rootstocks, with GN15 and GF677 showing better tolerance than Bitter Almond, although all rootstocks experienced reduced growth under salinity stress. However, the significant decline in Vialfas' performance at 75 mM NaCl suggests a possible threshold effect in its salt tolerance mechanisms. This pattern resembles the biphasic model of salt stress response described by Munns and Tester [49], where plants initially respond to the osmotic component of salt stress, followed by a response to ionic stress at higher salinity levels.

Guara's remarkable resilience pattern, particularly its improved performance at 75 mM NaCl after showing reduced growth at 25 mM and 50 mM NaCl, suggests the presence of inducible salt tolerance mechanisms. Similar phenomena have been observed in other plant species, such as certain halophytes, where high salinity triggers the activation of specific stress response pathways [53]. The gradual decline in Avijor's trunk diameter growth with increasing salinity levels indicates a linear response to salt stress. Reduced growth under salinity is likely due to various physiological responses and the additional energy costs associated with stress. Plants must allocate energy among maintenance, growth, and stress defense mechanisms, with salt stress limiting the total energy available through lowered photosynthesis [56]. Penta's stable performance across all salinity treatments contrasts with the typical plant response described by Kozłowski and Pallardy [57], where stress usually reduces growth as plants redirect energy from growth to stress defense mechanisms.

4.1.3. Shoot Length

The overall trend of decreasing growth rates and increasing variability with rising salinity levels across all genotypes is consistent with the general effects of salt stress on plants, as reviewed by Munns and Termaat [58].

The superior performance of Vialfas under control and mild stress conditions suggests a complex stress response mechanism that may reflect phenotypic plasticity, a trait often associated with adaptive potential in variable environments [59]. The significant decline at 75 mM NaCl observed in Avijor, which demonstrated good growth under control and mild stress conditions, exemplifies the concept of a salinity threshold tolerance described by Munns and Tester [49]. Similar threshold responses have been observed in other *Prunus* species, such as in various almond rootstocks [48], indicating a common but variable

trait within the genus. Guara's consistent intermediate performance across lower salinity treatments, coupled with its reduced adaptability to high salinity, reflects a moderate salt tolerance strategy. Penta's consistently slower growth under control and low salinity, but its improved performance under high-salinity stress, suggests a trade-off between growth potential and stress tolerance. This supports the 'stress tolerance syndrome' hypothesis, which proposes that stress-adaptive traits come at the cost of reduced growth under favorable conditions [60]. Plants show variable responses to salinity stress, with initial osmotic adjustments followed by negative ionic effects once tolerance thresholds are exceeded. The timing and severity of these thresholds vary significantly between species and genotypes [61,62].

4.2. Physiological Responses to Salinity Stress

4.2.1. Chlorophyll Fluorescence Parameters

As salinity increased from control to 75 mM NaCl, all genotypes exhibited decreased photosynthetic and electron flow parameters, consistent with the known effects of salt stress on Photosystem II (PSII) efficiency [49].

The observed decrease in the maximum quantum yield of PSII (F_v/F_m) under salt stress indicates damage to PSII reaction centers, aligning with the work of Ranjbarfordoei et al. [63] on almond trees (sweet almond). This decrease is attributed to the interference of salt ions in osmotic balance and the generation of oxidative stress. The energy capture efficiency (F_v/F_0) also decreased, suggesting damage to reaction centers and a compromised overall photosynthetic capacity, consistent with findings by Jimenez et al. [64]. The primary quantum efficiency of PSII ($\phi(Po)$) declined under salt stress, indicating reduced light energy utilization, consistent with studies by Acosta-Motos et al. [65] on two ornamental plant species, *Eugenia myrtifolia* Cambess. and *Myrtus communis* L.

The energy absorption capacity, measured by the area parameter, showed significant changes between measurements in April and September, indicating physiological adjustments to seasonal or salt stress conditions [65]. The normalized area (S_m), which indicates the size of the PSII electron acceptor pool, decreased under high salinity, suggesting reduced electron flow capacity [64]. The number of active PSII reaction centers (N) decreased under salt stress, indicating fewer functional centers, likely due to damage to the oxygen-evolving complex and other components of PSII [66].

Electron transfer efficiency from PSII to PSI (RE_o/RC) decreased under salinity, suggesting that salt stress affects the final electron transport phase. This effect is similar to those observed by [67], who noted similar impacts on PSII photochemistry under drought stress in sweet cherry cultivars. The F_0/F_m ratio, which measures the proportion of light energy not efficiently used in PSII, increased under salt stress, indicating greater energy dissipation as heat [63]. The variable J (V_j) in the OJIP curve increased under salt stress, indicating issues in electron transfer in sweet cherry cultivars [64].

Energy dissipation per reaction center (DI_o/RC) increased under saline conditions, suggesting a defense mechanism against excess energy. The Penta and Avijor genotypes maintained relatively stable photosynthetic yield (PI_{abs}) and electron flow (RE_o/RC), while Guara and Vialfas showed significant reductions. This differential response aligns with findings by Acosta-Motos et al. [65], who observed similar variability in salt tolerance among ornamental plants.

The decrease in PI_{abs} and F_v/F_m with increasing salinity, particularly in sensitive varieties, indicates a reduction in PSII efficiency and overall photosynthetic capacity [68]. The near collapse of electron flow (RE_o/RC and $\psi(E_o)$) in Guara at 75 mM NaCl suggests severe disruption of the electron transport chain, a common consequence of high salinity [69]. The partial recovery shown by Penta and Avijor at moderate salinities (25–50 mM NaCl) in

September suggests potential seasonal adaptation or acclimation processes. This adaptive capacity, which is absent in sensitive varieties, may involve osmotic adjustment or ion compartmentalization mechanisms [70].

4.2.2. Gas Exchange

In the control conditions, the genotypes exhibited distinct patterns of stomatal conductance, with Penta showing the highest peak conductance. This variability in baseline stomatal behavior aligns with findings from other *Prunus* species. For instance, Jimenez et al. [64] observed significant differences in stomatal conductance among various *Prunus* rootstocks under non-stress conditions, attributing these differences to genetic variability in water use efficiency. The high conductance exhibited by Penta under control conditions suggests a potential for higher photosynthetic capacity, which could be advantageous in optimal growing environments.

As salinity stress increased across treatments (25 mM to 75 mM NaCl), all genotypes exhibited decreased stomatal conductance, though to varying degrees. This response is consistent with the physiological strategy of stomatal closure under salt stress, which helps reduce water loss and prevent ion accumulation in leaf tissues [49,71].

Penta's dramatic reduction in stomatal conductance under severe stress (75 mM NaCl) after maintaining high conductance in lower stress conditions exemplifies the concept of salinity tolerance thresholds. This pattern is reminiscent of the findings by Läuchli and Grattan [72] in their study of various plant species and crops, particularly annual crops and cereals. Vialfas, in contrast, demonstrated a more conservative stomatal response across all treatments, maintaining relatively stable, albeit lower, conductance levels. While this approach may limit growth potential under optimal conditions, it could confer an advantage in consistently stressful environments, as suggested by Hochberg et al. [73] in their work on grapevine cultivars. The intermediate responses of Guara and Avijor, with Guara generally maintaining higher stomatal conductance under stress, suggest different osmotic adjustment strategies. Guara's ability to maintain relatively higher gas exchange under saline conditions could indicate more effective ion compartmentalization or osmolyte accumulation, mechanisms that have been associated with enhanced salt tolerance in Bitter Almond rootstock compared to Garnem [47].

4.2.3. Chlorophyll Content Analysis by Soil-Plant Analysis Development (SPAD)

The consistently higher SPAD values exhibited by Guara in the control treatment suggest a genotype-specific trait that could be linked to higher photosynthetic potential or structural differences in leaf tissue. Differences in SPAD values among species appear to be influenced by both genetic and environmental factors. Atar et al. [74] demonstrated that species can show distinctive chlorophyll content patterns, with significant variations among different tree and shrub species even under identical environmental conditions.

As salinity stress increased from 25 to 75 mM NaCl, genotype-specific responses became more pronounced, revealing diverse strategies for chlorophyll content maintenance under adverse conditions. Guara's ability to maintain high SPAD values—and even show increases under severe stress (75 mM NaCl)—is particularly noteworthy. This response parallels the findings by Acosta-Motos et al. [65] in *E. myrtifolia*, where increased SPAD values under salt stress were associated with leaf morphological adaptations such as increased thickness, which improved CO₂ diffusion to chloroplasts.

The stability of SPAD values observed in Penta across stress levels, particularly its lower values under high stress (75 mM NaCl), suggests a different adaptive strategy. This pattern is reminiscent of the findings by Munns and Tester [49], who reviewed various salinity tolerance mechanisms and noted that some plants maintain stable chlorophyll

levels as a conservative growth strategy under stress. However, it is important to note that while chlorophyll content can be indicative of photosynthetic capacity, the relationship between these parameters under salt stress may be species-dependent. Stepien and Johnson [75] found that salt-tolerant *Thellungiella* maintained both chlorophyll content and photosynthetic efficiency under salt stress, while salt-sensitive *Arabidopsis* showed declines in both parameters.

The intermediate responses of Avijor and Vialfas, characterized by generally increasing SPAD values over time, even under stress, indicate a degree of resilience in chlorophyll content maintenance. This capacity for chlorophyll accumulation under saline conditions has been associated with salt tolerance in other species. Ashraf and Harris [76] noted in their review of physiological markers of salinity tolerance that chlorophyll accumulation as an indicator of salt tolerance should be considered on a species-specific basis.

4.3. Visual Salinity Stress Symptoms

All genotypes exhibited progressive reductions in plant height, leaf number, leaf health, and root development as salinity increased, illustrating the cumulative negative effects of salt stress on plant growth and development. This pattern is consistent with the findings by Dejampour et al. [77] in their study on peach rootstocks.

The observed differences in salt tolerance among the studied genotypes corroborate findings from other *Prunus* studies. For instance, Zrig et al. [47] reported significant variability in salt tolerance among almond rootstocks, with some genotypes maintaining superior growth and physiological parameters under saline conditions. Similarly, Rahnesan et al. [78] observed differential responses to salt stress among pistachio genotypes, highlighting the genetic basis of salt tolerance in other woody perennial species beyond *Prunus*.

The superior performance of Guara and Penta under moderate salinity levels (25–50 mM NaCl) suggests the presence of effective salt tolerance mechanisms in these genotypes. This aligns with findings by Momenpour and Imani [79], who identified variability in salt tolerance among almond cultivars (Rabie, Perless, Super Nova, D99, 1–16, and 8–24), with D99 maintaining higher growth and ion homeostasis under saline conditions. The mechanisms underlying this enhanced tolerance could involve more efficient Na⁺ exclusion, improved K⁺/Na⁺ selectivity, or enhanced ion compartmentalization, as suggested by Munns and Tester [49].

The identification of a critical salinity threshold around 50 mM NaCl, where stress symptoms became more severe, is consistent with observations in other *Prunus* studies. Dejampour et al. [77] reported a significant decline in photosynthetic efficiency and growth parameters in peach rootstocks (HS314, HS312, GF 677, HS 302) at salinity levels of 6 and 9 dS m⁻¹.

The severe impact at 75 mM NaCl, particularly evident in Avijor, suggests that this concentration exceeds the tolerance threshold of these *Prunus* genotypes. This finding is consistent with research by Toro et al. [50] on salt stress in *Prunus* rootstocks, which showed that Mariana 2624 and Garnem are more resistant than Mazzard F12/1 and Cab6P at 120 mM NaCl.

The differential responses observed in leaves, stems, and roots provide insights into organ-specific salt stress adaptations. The high sensitivity of leaves to salt stress, evidenced by progressive chlorosis and necrosis, highlights that these symptoms are typically caused by excessive Cl⁻ content in leaves, while Na⁺ tends to accumulate in roots, trunk, and branches, aligning with observations by Zrig et al. [47] in almond cultivars (Garnem and Bitter Almond).

This sensitivity in leaves likely reflects the accumulation of toxic ions in photosynthetic tissues; high concentrations of both Na^+ and Cl^- in leaf tissues can reduce photosynthetic capacity. Chlorophyll degradation, specifically linked to high Cl^- accumulation, was described by Tavakkoli et al. [80].

The deterioration of the root system with increasing salinity was noteworthy across all genotypes, especially in Avijor, and directly impacted water and nutrient uptake. This observation is consistent with the findings by Sandhu et al. [48], who reported significantly reduced survival rates and root biomass in salt-stressed *Prunus* rootstocks; the Na-Cl dominant treatment (120 mM NaCl) caused the most severe reductions in root growth.

The maintenance of better root development in Guara and Penta under moderate salinity suggests more effective root-based salt tolerance mechanisms, possibly involving enhanced ion exclusion or sequestration strategies. As described by Flowers and Colmer [81], species differ in their ability to restrict ion transport from roots to shoots and vary in their capacities for ion compartmentalization.

4.4. Changes in Mineral Content Under Salinity Stress

4.4.1. Calcium Content and Distribution

Calcium distribution varied among plant organs and genotypes, with roots consistently showing the highest levels. This aligns with the findings by Zrig et al. [47] and may mitigate Na^+ toxicity by maintaining membrane integrity and regulating ion channels [82]. In some plants, maintaining high Ca^{2+} content under salinity is associated with salt tolerance. However, for almond rootstocks, no clear association was found between tissue Ca^{2+} concentration and salinity tolerance [48]. Leaf Ca^{2+} content decreased with increasing salinity, yet Dejampour et al. [77] found no significant changes in leaf Ca^{2+} concentrations or $\text{Na}^+/\text{Ca}^{2+}$ ratios under salt stress in *P. dulcis* rootstocks. Wood Ca^{2+} levels displayed complex dynamics, while stem Ca^{2+} content remained low, contrasting with its role in salt tolerance in other tree species [83].

Regarding genotype influence, the high calcium levels in Avijor roots suggest a potential salt tolerance mechanism, as Ca^{2+} helps maintain membrane integrity and regulate ion transport under saline conditions [84]. However, Avijor's variable response to salinity suggests there may be a threshold for its tolerance. Guara exhibited consistently high Ca^{2+} levels across treatments, especially in leaves, suggesting an efficient Ca^{2+} transport system and robust homeostasis mechanism, which may contribute to salt tolerance. This pattern is similar to the findings in pistachio, where high Ca^{2+} levels are linked to enhanced salt tolerance [78].

Penta's lower Ca^{2+} levels may indicate a less effective uptake or distribution system, potentially increasing susceptibility to salt-induced calcium deficiencies. Vialfas showed moderate Ca^{2+} levels with minimal variability, especially in wood tissue, possibly indicating a balanced partitioning strategy associated with improved salt tolerance. Rengel [82] demonstrated that genotypic variation in calcium management includes efficiency of Ca^{2+} use, capacity for Ca^{2+} uptake and transport, and maintenance of Ca^{2+} homeostasis during salt stress.

4.4.2. Potassium Accumulation Patterns

Potassium distribution varied markedly across plant organs, with organ-specific responses to salinity observed in terms of ion accumulation. This differential response across organs underscores the complexity of whole-plant K^+ homeostasis under stress conditions—a concept explored by Anschutz et al. [85] in their study on potassium regulation mechanisms.

Leaves consistently showed the highest K^+ content, a pattern consistent with the findings of Zrig et al. [47], reflecting potassium's essential roles in different plant tissues, particularly in stomatal regulation and photosynthesis [86]. The substantial decrease in leaf K^+ content under salinity stress aligns with studies attributing this to both reduced K^+ uptake and increased K^+ efflux under saline conditions [85]. The relatively high K^+ levels maintained in roots at 75 mM NaCl may be a mechanism to support K^+/Na^+ homeostasis, a key factor in salt tolerance. The ability to retain K^+ within cells may be crucial for salt tolerance, as proposed by Shabala and Cuin [87].

Avijor showed a steady decrease in K^+ content across treatments, whereas Penta maintained slightly higher K^+ levels, especially at higher salinity levels. This suggests a potential mechanism for better K^+ retention under high salinity conditions [82]. Vialfas exhibited the highest mean K^+ content under control conditions but showed significant reductions as salinity increased. Guara displayed similar trends, with its K^+ content reaching the lowest level among all genotypes at 75 mM NaCl. These varied responses highlight the genetic diversity in salt tolerance mechanisms within *Prunus* species. As noted by Shabala and Cuin [87], over 80% of the genetic variability in salt tolerance may relate to a single physiological trait: a cell's ability to prevent NaCl-induced K^+ leakage.

4.4.3. Chloride Accumulation and Distribution

Salt-tolerant genotypes of citrus and grapevine with low shoot Cl^- concentrations have higher root Cl^- concentrations compared to sensitive genotypes, suggesting a more efficient Cl^- compartmentalization in root vacuoles. In some avocado rootstocks, higher leaf Cl^- concentrations are associated with salt tolerance, potentially indicating effective Cl^- sequestration in leaf vacuoles [88].

Leaves consistently showed the highest Cl^- content, followed by roots, stems, and wood. This pattern is consistent with findings by Papadakis et al. [89] in *Prunus cerasus* L., where leaves accumulated the highest Cl^- levels under salt stress. Such substantial Cl^- accumulation in leaves can lead to ionic toxicity and impaired photosynthetic efficiency. This preferential Cl^- accumulation in leaves may act as a protective mechanism for more sensitive organs or help maintain osmotic balance, as proposed by Munns and Tester [49] for glycophytes under salt stress. Considering genotype-specific responses, Vialfas and Avijor accumulated more Cl^- in leaves than Penta and Guara. These differences may be due to variations in root-to-shoot Cl^- transport efficiency or vacuolar sequestration capacity, as suggested by Teakle and Tyerman [88] in their study on Cl^- transport in plants.

The pronounced genotype-specific responses at higher salt concentrations, particularly the distinct grouping of Avijor and Guara as separate from Penta and Vialfas at 50 mM NaCl, suggest differential activation of salt tolerance mechanisms. This observation aligns with Sandhu et al. [48], who reported varied physiological responses among 14 commercial almond rootstocks at different salinity levels. At 75 mM NaCl, Avijor exhibited the highest mean Cl^- content, followed closely by Vialfas, suggesting that these genotypes may be Cl^- includers. Similar variability in Cl^- accumulation was observed by Dejampour et al. [77] in *Prunus* rootstocks under saline conditions, where maximum Cl^- accumulation was reported in the Sahand and GF677 genotypes. The consistently lower Cl^- accumulation in Penta across all organs, particularly at higher salinity levels, suggests possible differences in salt tolerance mechanisms, similar to findings reported in GF677 and MRS2 *Prunus* rootstocks grafted on peach (cv. Armking) [90].

4.4.4. Sodium Content and Distribution

Sodium distribution varied substantially across plant organs, with leaves showing the highest Na^+ content, followed by roots, stems, and wood. This pattern aligns with findings

by Momenpour and Imani [79] in *Prunus* rootstocks. The preferential accumulation of Na^+ in leaves may serve to protect more sensitive organs or assist in maintaining osmotic balance, as proposed by Munns and Tester [49] and Hasegawa [84] for glycophytes under salt stress. Such preferential Na^+ accumulation has been observed in other woody species, suggesting it may be a common strategy in glycophytes [56,91].

The consistent trend of the highest Na^+ levels in leaves across all genotypes might indicate a strategy of Na^+ compartmentalization in leaves to protect other organs or could reflect the movement of Na^+ through the transpiration stream to the leaves. However, substantial Na^+ accumulation in leaves can result in ionic toxicity and impaired photosynthetic efficiency, as El Yamani and Cordovilla [92] observed in olive trees. These Na^+ accumulation patterns suggest multiple strategies for managing salt stress, including selective ion transport, Na^+ compartmentalization in leaves, and possibly Na^+ exclusion at the root level [53,93].

Genotypic differences in Na^+ distribution were observed, with Avijor accumulating more Na^+ in leaves and Vialfas showing higher Na^+ content in roots. Such differences could arise from variations in root-to-shoot Na^+ transport efficiency or vacuolar sequestration capacity [86,94]. In Avijor, differential Na^+ accumulation according to salinity treatment aligns with previous research on *Prunus* rootstocks, where substantial variability in ion accumulation has been noted among cultivars and rootstocks [48]. Penta's consistently lower Na^+ accumulation, especially at 50 mM NaCl, suggests potentially unique salt tolerance mechanisms, as also reported in other *Prunus* species [89].

It is noteworthy that genotype-specific responses became more pronounced under higher salt stress, particularly at 50 mM NaCl, suggesting that moderate salinity may be optimal for identifying salt-tolerant genotypes. However, the convergence of responses at 75 mM NaCl suggests a potential threshold effect, a phenomenon observed in other *Prunus* spp. studies [47,50].

4.4.5. Potassium/Sodium Ratio

Guara and Penta's superior ability to maintain higher K^+/Na^+ ratios under salt stress is noteworthy and aligns with observations by Papadakis et al. [89] in almond cultivars, where salt-tolerant genotypes demonstrated better K^+/Na^+ homeostasis.

Genetic variation influences the ability to maintain favorable K^+/Na^+ ratios, which is crucial for salt tolerance. Preferential K^+ accumulation in leaves is a well-documented strategy in many plant species to mitigate sodium's detrimental effects on photosynthetic machinery [49]. The relatively stable K^+/Na^+ ratios observed in wood and stem tissues suggest a potential buffering role in ion homeostasis, as noted in olive trees by El Yamani and Cordovilla [92]. Maintaining consistent ion ratios in woody tissues could be essential for long-term salt tolerance in tree species, potentially protecting vital transport systems and meristematic regions from ionic imbalances.

4.4.6. Calcium/Sodium Ratio

Genotypic variations in $\text{Ca}^{2+}/\text{Na}^+$ ratio maintenance under saline conditions, especially the strong performance of Guara, indicate diverse salt tolerance mechanisms within the *Prunus* species. These differences likely originate from variations in ion transport systems, as suggested by Shabala and Cuin [87]. Guara's superior performance could be due to more efficient Na^+ exclusion mechanisms or enhanced Ca^{2+} uptake systems, similar to those found in salt-tolerant varieties of other species [49]. The consistently higher $\text{Ca}^{2+}/\text{Na}^+$ ratios observed in roots across all genotypes support the idea that roots serve as a critical first line of defense against salt stress. This pattern suggests the presence of efficient ion selectivity mechanisms in root tissues, possibly involving selective ion trans-

porters similar to those described by Shabala [95]. The sharp decrease in leaf $\text{Ca}^{2+}/\text{Na}^{+}$ ratios with increasing salinity highlights the vulnerability of photosynthetic tissues to ionic imbalances. This finding aligns with Munns and Gilliam [56], who emphasize the importance of maintaining favorable ion ratios in leaves to preserve photosynthetic capacity under salt stress. Genotypic differences in leaf $\text{Ca}^{2+}/\text{Na}^{+}$ ratios, especially the higher ratios maintained by Guara, may be linked to variations in ion compartmentalization strategies or differences in xylem loading and unloading processes, as described by Rengel [82].

4.5. Genotype Performance Comparison

The four almond genotypes exhibited distinct responses to increasing salinity, revealing varying levels of salt tolerance.

Guara demonstrated the best overall performance under saline conditions. It maintained growth and physiological functions across salinity levels, showing particular resilience in trunk diameter and fresh weight. Guara's salt tolerance was underpinned by its ability to maintain high Ca^{2+} levels and favorable ion ratios under stress. Penta ranked a close second in salt tolerance. While not showing the highest vigor under control conditions, Penta exhibited remarkable stability across all salinity treatments. It maintained stable photosynthetic yield and electron transport under stress and showed effective Na^{+} exclusion and Cl^{-} regulation. This consistent performance suggests robust salt tolerance mechanisms. Vialfas showed good performance under low-to-moderate salinity but higher sensitivity to severe salt stress. It demonstrated superior vigor under control and low salinity conditions, particularly in growth parameters. However, Vialfas experienced significant declines at 75 mM NaCl, indicating a lower threshold for severe salt stress. Avijor proved the most sensitive to salt stress among the four genotypes. It showed significant declines in growth parameters at moderate-to-high salinity levels (25 and 50 mM NaCl) and struggled to maintain physiological performance under high salinity (75 mM NaCl). Avijor's sensitivity was further evidenced by high Na^{+} accumulation in leaves, suggesting less effective Na^{+} exclusion mechanisms.

In terms of overall salt tolerance, the genotypes can be ranked as Guara > Penta > Vialfas > Avijor. This ranking considers both absolute performance under high salinity and stability of response across stress levels.

4.6. Management Framework and Practical Applications

4.6.1. Integrated Management Framework for Salinity Stress

While our study focuses on genotype selection, optimizing almond production under saline conditions requires an integrated approach (Figure 10). The framework presented illustrates how different management strategies interact to achieve improved yields under saline conditions. Genetic management through appropriate cultivar selection—as investigated in this study—forms one of the four key pillars, alongside water management, soil management, and continuous monitoring.

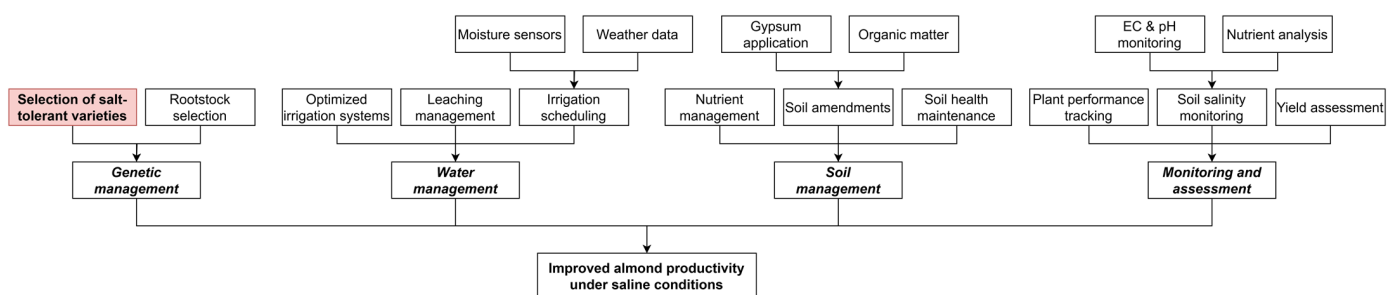


Figure 10. Management framework for almond cultivation under saline conditions.

Soil health assessment plays a crucial role in this integrated approach, particularly for managing saline conditions. It involves analyzing physical, chemical, and biological soil properties, with key indicators such as electrical conductivity (EC), pH, and sodium adsorption ratio (SAR) used to identify and monitor salt-affected areas. While general soil health monitoring tools have shown success in agricultural management [96], managing almond orchards under saline conditions requires particular attention to these salinity-specific parameters. Our results demonstrate that monitoring these indicators provides crucial information for adjusting management practices.

Management strategies guided by soil assessment include applying gypsum to improve soil structure and enhance salt leaching, optimizing irrigation methods through drip systems and appropriate leaching fractions, and incorporating organic matter to boost microbial activity and nutrient availability. Advanced monitoring tools like sensors and GIS technology enable continuous soil assessment, ensuring precise, timely adjustments to these interventions. This holistic approach allows growers to maximize the benefits of salt-tolerant genotypes while maintaining soil health and ensuring long-term orchard sustainability.

4.6.2. Genotype-Specific Applications

The differential salt tolerance observed among the four almond genotypes has significant implications for orchard management and breeding programs, particularly in regions facing increasing soil salinization.

For areas with salinity levels of up to 50 mM NaCl, Guara emerges as the optimal choice due to its consistent performance across various stress levels. Its ability to maintain growth and physiological functions under saline conditions makes it suitable for a wide range of environments, potentially increasing orchard resilience to fluctuating soil salinity.

In regions prone to higher salinity levels or where salinity may increase over time, Penta could be the preferred option. Its stable performance across all salinity treatments, including severe stress conditions, suggests it may be better equipped to handle long-term exposure to high salinity. Penta's effective ion regulation mechanisms could be particularly valuable in these challenging environments.

Vialfas, with its superior vigor under low-salinity conditions, could be an excellent choice for areas with mild salinity issues or as part of a breeding program aimed at combining its vigorous growth traits with the salt tolerance mechanisms of Guara or Penta.

While Avijor showed the highest sensitivity to salt stress, its traits could still be valuable in breeding programs. Understanding the mechanisms behind its sensitivity could provide insights into key genes or processes involved in salt tolerance, potentially leading to the development of even more resilient cultivars.

These findings also highlight the importance of soil and water salinity assessment and monitoring in orchard management. The observed genotype-specific salinity thresholds can guide irrigation strategies and soil amendment practices, helping to maintain optimal growing conditions for each cultivar.

For breeding programs, these results provide a foundation for developing new, salt-tolerant almond varieties. Cross-breeding between Guara or Penta and other high-yielding varieties could potentially result in cultivars that combine superior salt tolerance with other desirable agronomic traits.

In short, the selection of almond genotypes should be tailored to specific environmental conditions and management goals. This study provides valuable insights for such decision making, potentially contributing to more sustainable and productive almond cultivation in the face of increasing soil salinization.

5. Conclusions

This study of four self-rooted almond genotypes (Vialfas, Guara, Penta, and Avijor) under varying salinity levels revealed genotype-specific responses to salt stress across different plant organs and physiological processes. All genotypes exhibited a critical salinity threshold between 50 and 75 mM NaCl, beyond which significant deterioration in growth and physiological parameters occurred. Guara and Penta demonstrated superior overall performance under saline conditions, maintaining better growth, physiological functions, and ion homeostasis across salinity treatments. These genotypes showed more effective mechanisms for maintaining favorable K^+/Na^+ and Ca^{2+}/Na^+ ratios, particularly in leaves and roots, which appeared to be crucial for their salt tolerance.

These findings have significant implications for almond cultivation in regions affected by soil or water salinization. The observed genotype-specific responses provide valuable guidance for selecting plant material in super-high-density, self-rooted almond orchards—a cost-effective alternative for regions facing water scarcity and salinity challenges, whether transitioning from traditional almond orchards or cereal crops. Furthermore, the identified salt-tolerant genotypes, particularly Guara and Penta, show considerable promise as breeding stock for developing more resilient almond varieties.

Future research should include long-term field studies to assess the performance of these genotypes under variable environmental conditions, as salt tolerance can be influenced by other abiotic factors. Investigation of the molecular and genetic basis of the observed differences in salt tolerance could facilitate marker-assisted selection in breeding programs. Evaluation of the impact of salt stress on fruit yield and quality in these genotypes would also be valuable for commercial almond production.

Supplementary Materials: The following supporting information can be downloaded at: <https://www.mdpi.com/article/10.3390/agriculture15030254/s1>, Figure S1. Box-plot and statistical data for fresh weight as a function of the treatment \times organ interaction, with values pooled across all four genotypes for each treatment–organ combination; Figure S2. Box-plot for fresh weight as a function of the treatment \times organ \times genotype interaction; Figure S3. Box-plot and statistical data for total plant fresh weight as a function of the genotype \times treatment interaction; Figure S4. Box-plot and statistical data for dry weight as a function of the treatment \times organ interaction, with values pooled across all four genotypes for each treatment–organ combination; Figure S5. Box-plot for dry weight as a function of the treatment \times organ \times genotype interaction; Figure S6. Box-plot and statistical data for total plant dry weight as a function of the genotype \times treatment interaction; Figure S7. Overall efficiency of photosystem II; Figure S8. Energy and electron transport; Figure S9. Energy dissipation and damage; Figure S10. Box-plot and statistical data for Ca^{2+} as a function of the treatment \times organ interaction; Figure S11. Box-plot and statistical data for Ca^{2+} as a function of the genotype \times organ interaction; Figure S12. Box-plot and statistical data for Ca^{2+} as a function of the genotype \times treatment interaction; Figure S13. Box-plot and statistical data for K^+ as a function of the treatment \times organ interaction; Figure S14. Box-plot and statistical data for K^+ as a function of the genotype \times organ interaction; Figure S15. Box-plot and statistical data for K^+ as a function of the genotype \times treatment interaction; Figure S16. Box-plot and statistical data for Cl^- as a function of the treatment \times organ interaction; Figure S17. Box-plot and statistical data for Cl^- as a function of the genotype \times organ interaction; Figure S18. Box-plot and statistical data for Cl^- as a function of the genotype \times treatment interaction; Figure S19. Box-plot and statistical data for Na^+ as a function of the treatment \times organ interaction; Figure S20. Box-plot and statistical data for Na^+ as a function of the genotype \times organ interaction; Figure S21. Box-plot and statistical data for Na^+ as a function of the genotype \times treatment interaction; Figure S22. Box-plot and statistical data for K^+/Na^+ as a function of the treatment \times organ interaction; Figure S23. Box-plot and statistical data for K^+/Na^+ as a function of the genotype \times organ interaction; Figure S24. Box-plot and statistical data for K^+/Na^+ as a function of the genotype \times treatment interaction; Figure S25. Box-plot and statistical data for Ca^{2+}/Na^+ as

a function of the treatment \times organ interaction; Figure S26. Box-plot and statistical data for $\text{Ca}^{2+}/\text{Na}^{+}$ as a function of the genotype \times organ interaction; Figure S27. Box-plot and statistical data for $\text{Ca}^{2+}/\text{Na}^{+}$ as a function of the genotype by treatment interaction; Table S1. Spline data for the effects of genotype and treatment combinations on trunk diameter; Table S2. Spline data for the effects of genotype and treatment combinations on shoot length; Table S3. Descriptive statistics of fluorimeter measurements; Table S4. Spline data for the effects of genotype and treatment combinations on stomatal conductance; Table S5. Spline data for the effects of genotype and treatment combinations on SPAD values; Table S6. Descriptive statistics and robustness analysis of ion concentrations, biomass parameters, and ion ratios in plant tissue samples; Table S7. ANOVA of the models $\log(\text{variable})$ p -values of each of the factors along with their interactions; Table S8. Robust comparisons of the group p -values of each of the factors along with their interactions.

Author Contributions: Conceptualization, X.R.-G., J.C.-G. and P.M.-R.; methodology, M.V.-M., J.C.-G., L.A.-R., R.Z.-G. and P.M.-R.; software, L.A.-R.; validation, J.C.-G. and R.Z.-G.; formal analysis, X.R.-G., M.V.-M., J.C.-G., L.A.-R. and P.M.-R.; investigation, X.R.-G., M.V.-M., J.C.-G., R.Z.-G. and P.M.-R.; resources, X.R.-G.; data curation, L.A.-R.; writing—original draft preparation, X.R.-G., M.V.-M., J.C.-G., L.A.-R. and P.M.-R.; writing—review and editing, X.R.-G. and P.M.-R.; visualization, X.R.-G., J.C.-G. and L.A.-R.; supervision, M.V.-M. and J.C.-G. All authors have read and agreed to the published version of the manuscript.

Funding: This research received no external funding.

Institutional Review Board Statement: Not applicable.

Data Availability Statement: All data supporting the findings of this study are available within the paper and its Supplementary Information. Should any raw data files be needed in another format, they are available from the corresponding author upon reasonable request.

Conflicts of Interest: Author Xavier Rius-Garcia was employed by the company Agromillora Group. All authors declare that the research was conducted in the absence of any commercial or financial relationships that could be construed as potential conflicts of interest.

References

1. International Nut & Dried Fruit. *Nuts & Dried Fruits Statistical Yearbook 2019/2020*; International Nut & Dried Fruit: Reus, Spain, 2021; p. 80.
2. FAOSTAT. Food and Agricultural Commodities Production. Available online: <http://www.fao.org/faostat/en/#data/QC/visualize> (accessed on 20 January 2025).
3. Industry Research. *Global Almond Industry Research Report 2023. Competitive Landscape, Market Size, Regional Status, and Prospect*; Absolute Reports Pvt. Ltd.: Maharashtra, India, 2023; p. 111.
4. Spanish Ministry of Agriculture Fisheries and Food. *Frutos Secos: Análisis de la Realidad Productiva 2021*; Spanish Ministry of Agriculture, Fisheries and Food: Madrid, Spain, 2022; p. 60.
5. Felipe, A.J.; Rius, X.; Rubio-Cabetas, M.J. *El Cultivo del Almendro. El Almendro II*; Calidad Gráfica Araconsa SL: Zaragoza, Spain, 2022; p. 568.
6. Sottile, F.; Barone, E.; Barbera, G.; Palasciano, M. The Italian almond industry: New perspectives and ancient tradition. *Acta Hort.* **2014**, *1028*, 401–407. [[CrossRef](#)]
7. Expósito, A.; Berbel, J. The economics of irrigation in almond orchards. Application to southern Spain. *Agronomy* **2020**, *10*, 796. [[CrossRef](#)]
8. Maldera, F.; Vivaldi, G.A.; Iglesias-Castellarnau, I.; Camposeo, S. Two almond cultivars trained in a super-high density orchard show different growth, yield efficiencies and damages by mechanical harvesting. *Agronomy* **2021**, *11*, 1406. [[CrossRef](#)]
9. Caruso, T.; Campisi, G.; Marra, F.P.; Camposeo, S.; Vivaldi, G.A.; Proietti, P.; Nasini, L. Growth and yields of 'Arbequina' high-density planting systems in three different olive growing areas in Italy. *Acta Hort.* **2014**, *1057*, 341–348. [[CrossRef](#)]
10. Connor, D.J.; Gómez-del-Campo, M.; Rousseaux, M.C.; Searles, P.S. Structure, management and productivity of hedgerow olive orchards: A review. *Sci. Hort.* **2014**, *169*, 71–93. [[CrossRef](#)]
11. Pellegrini, G.; Sala, P.L.; Camposeo, S.; Contò, F. Economic sustainability of the olive oil high and super-high density cropping systems in Italy. *Glob. Bus. Econ. Rev.* **2017**, *19*, 553–569. [[CrossRef](#)]

12. Pellegrini, G.; Ingraio, C.; Camposeo, S.; Tricase, C.; Contò, F.; Huisinigh, D. Application of water footprint to olive growing systems in the Apulia region: A comparative assessment. *J. Clean. Prod.* **2016**, *112*, 2407–2418. [CrossRef]
13. Agromillora. Super High-Density Almond Crops. Available online: <https://www.agromillora.com/innovation/super-high-density-system/almonds-in-super-high-density/> (accessed on 20 January 2025).
14. Dias, A.B.; Caeiro, L.; Félix, G.; Falcão, J.M. Evaluation of biometric parameters of ‘Belona’, ‘Guara’ and ‘Lauranne’ cultivars in a superhigh density orchard. *Acta Hort.* **2018**, *1219*, 73–78. [CrossRef]
15. Iglesias, I. Sistemas de plantación 2D: Una novedad en almendro, una realidad en frutales. Hacia una alta eficiencia. *Rev. Frutic.* **2019**, *67*, 22–44.
16. Ben Yahmed, J.; Ghrab, M.; Ben Mimoun, M. Eco-physiological evaluation of different scion-rootstock combinations of almond grown in Mediterranean conditions. *Fruits* **2016**, *71*, 185–193. [CrossRef]
17. Casanova-Gascón, J.; Figueras-Panillo, M.; Iglesias-Castellarnau, I.; Martín-Ramos, P. Comparison of SHD and open-center training systems in almond tree orchards cv. ‘Soleta’. *Agronomy* **2019**, *9*, 874. [CrossRef]
18. Phogat, V.; Mallants, D.; Cox, J.W.; Šimůnek, J.; Oliver, D.P.; Awad, J. Management of soil salinity associated with irrigation of protected crops. *Agric. Water Manag.* **2020**, *227*, 105845. [CrossRef]
19. Casanova-Gascón, J.; Martí-Dalmau, C.; Martín-Ramos, P. Comportamiento de variedades autorradicadas de almendro frente a factores limitantes del medio. *Olint Rev. Plantaciones Superintensiv. Olivo* **2020**, *36*, 31–34.
20. Hoagland, D.R.; Arnon, D.I. *The Water-Culture Method for Growing Plants Without Soil*; College of Agriculture-University of California; California Agricultural Experiment Station: Berkeley, CA, USA, 1950; p. 31.
21. Perica, S.; Goreta, S.; Selak, G.V. Growth, biomass allocation and leaf ion concentration of seven olive (*Olea europaea* L.) cultivars under increased salinity. *Sci. Hort.* **2008**, *117*, 123–129. [CrossRef]
22. Sapkota, Y.; McDonald, L.M.; Griggs, T.C.; Basden, T.J.; Drake, B.L. Portable X-ray fluorescence spectroscopy for rapid and cost-effective determination of elemental composition of ground forage. *Front. Plant Sci.* **2019**, *10*, 317. [CrossRef]
23. Antonangelo, J.; Zhang, H. Soil and plant nutrient analysis with a portable XRF probe using a single calibration. *Agronomy* **2021**, *11*, 2118. [CrossRef]
24. Towett, E.K.; Shepherd, K.D.; Lee Drake, B. Plant elemental composition and portable X-ray fluorescence (pXRF) spectroscopy: Quantification under different analytical parameters. *X-Ray Spectrom.* **2016**, *45*, 117–124. [CrossRef]
25. McGladdery, C.; Weindorf, D.C.; Chakraborty, S.; Li, B.; Paulette, L.; Podar, D.; Pearson, D.; Kusi, N.Y.O.; Duda, B. Elemental assessment of vegetation via portable X-ray fluorescence (pXRF) spectrometry. *J. Environ. Manag.* **2018**, *210*, 210–225. [CrossRef]
26. Singh, V.K.; Sharma, N.; Singh, V.K. Application of X-ray fluorescence spectrometry in plant science: Solutions, threats, and opportunities. *X-Ray Spectrom.* **2021**, *51*, 304–327. [CrossRef]
27. Jones, J.B.; Case, V.W. Sampling, handling, and analyzing plant tissue samples. In *Soil Testing and Plant Analysis*, 3rd ed.; Westerman, R.L., Ed.; Soil Science Society of America: Madison, WI, USA, 2018; Volume 3, pp. 389–427.
28. Kalra, Y. *Handbook of Reference Methods for Plant Analysis*; CRC Press: Boca Raton, FL, USA, 1997; p. 320. [CrossRef]
29. Kalaji, H.M.; Schansker, G.; Ladle, R.J.; Goltsev, V.; Bosa, K.; Allakhverdiev, S.I.; Brestic, M.; Bussotti, F.; Calatayud, A.; Dąbrowski, P.; et al. Frequently asked questions about in vivo chlorophyll fluorescence: Practical issues. *Photosynth. Res.* **2014**, *122*, 121–158. [CrossRef] [PubMed]
30. Stirbet, A.; Govindjee. On the relation between the Kautsky effect (chlorophyll a fluorescence induction) and Photosystem II: Basics and applications of the OJIP fluorescence transient. *J. Photochem. Photobiol. B* **2011**, *104*, 236–257. [CrossRef] [PubMed]
31. Strasser, R.J.; Tsimilli-Michael, M.; Srivastava, A. Analysis of the chlorophyll a fluorescence transient. In *Chlorophyll a Fluorescence: A Signature of Photosynthesis*; Papageorgiou, G.C., Govindjee, Eds.; Springer: Dordrecht, The Netherlands, 2004; pp. 321–362. [CrossRef]
32. R Core Team. In *R: A Language and Environment for Statistical Computing*; R Foundation for Statistical Computing: Vienna, Austria, 2021.
33. Lilliefors, H.W. On the Kolmogorov-Smirnov test for normality with mean and variance unknown. *J. Am. Stat. Assoc.* **1967**, *62*, 399–402. [CrossRef]
34. Shapiro, S.S.; Wilk, M.B. An analysis of variance test for normality (complete samples). *Biometrika* **1965**, *52*, 591–611. [CrossRef]
35. Brown, M.B.; Forsythe, A.B. Robust tests for the equality of variances. *J. Am. Stat. Assoc.* **1974**, *69*, 364. [CrossRef]
36. Kruskal, W.H.; Wallis, W.A. Use of ranks in one-criterion variance analysis. *J. Am. Stat. Assoc.* **1952**, *47*, 583–621. [CrossRef]
37. Wilcox, R.R. *Introduction to Robust Estimation and Hypothesis Testing*, 5th ed.; Academic Press: London, UK, 2021.
38. Welch, B.L. On the comparison of several mean values: An alternative approach. *Biometrika* **1951**, *38*, 330–336. [CrossRef]
39. Mond, C.E.D.; Lenth, R.V. A robust confidence interval for location. *Technometrics* **1987**, *29*, 211. [CrossRef]
40. Harrell, F.E. *Regression Modeling Strategies. With Applications to Linear Models, Logistic and Ordinal Regression, and Survival Analysis*, 2nd ed.; Springer: Cham, Switzerland; New York, NY, USA, 2015; p. 582. [CrossRef]
41. Friedman, J.H. Multivariate adaptive regression splines. *Ann. Stat.* **1991**, *19*, 1–67. [CrossRef]
42. Durrleman, S.; Simon, R. Flexible regression models with cubic splines. *Stat. Med.* **2006**, *8*, 551–561. [CrossRef]

43. Krzanowski, W.J. *An Introduction to Statistical Modelling*; Wiley: London, UK, 2010; p. 272.
44. Akaike, H. Information theory and an extension of the maximum likelihood principle. In *Selected Papers of Hirotugu Akaike*; Parzen, E., Tanabe, K., Kitagawa, G., Eds.; Springer: New York, NY, USA, 1998; pp. 199–213. [[CrossRef](#)]
45. Schwarz, G. Estimating the dimension of a model. *Ann. Stat.* **1978**, *6*, 461–464. [[CrossRef](#)]
46. Chen, J.; Chen, Z. Extended Bayesian information criteria for model selection with large model spaces. *Biometrika* **2008**, *95*, 759–771. [[CrossRef](#)]
47. Zrig, A.; Ben Mohamed, H.; Tounekti, T.; Khemira, H.; Serrano, M.; Valero, D.; Vadel, A.M. Effect of rootstock on salinity tolerance of sweet almond (cv. Mazzetto). *S. Afr. J. Bot.* **2016**, *102*, 50–59. [[CrossRef](#)]
48. Sandhu, D.; Kaundal, A.; Acharya, B.R.; Forest, T.; Pudussery, M.V.; Liu, X.; Ferreira, J.F.S.; Suarez, D.L. Linking diverse salinity responses of 14 almond rootstocks with physiological, biochemical, and genetic determinants. *Sci. Rep.* **2020**, *10*, 21087. [[CrossRef](#)] [[PubMed](#)]
49. Munns, R.; Tester, M. Mechanisms of salinity tolerance. *Annu. Rev. Plant Biol.* **2008**, *59*, 651–681. [[CrossRef](#)]
50. Toro, G.; Pimentel, P.; Salvatierra, A. Effective categorization of tolerance to salt stress through clustering *Prunus* rootstocks according to their physiological performances. *Horticulturae* **2021**, *7*, 542. [[CrossRef](#)]
51. Tattini, M.; Gucci, R.; Coradeschi, M.A.; Ponzio, C.; Everard, J.D. Growth, gas exchange and ion content in *Olea europaea* plants during salinity stress and subsequent relief. *Physiol. Plant.* **2006**, *95*, 203–210. [[CrossRef](#)]
52. Rewald, B.; Leuschner, C.; Wiesman, Z.; Ephrath, J.E. Influence of salinity on root hydraulic properties of three olive varieties. *Plant Biosyst.* **2011**, *145*, 12–22. [[CrossRef](#)]
53. Flowers, T.J.; Colmer, T.D. Salinity tolerance in halophytes. *New Phytol.* **2008**, *179*, 945–963. [[CrossRef](#)]
54. Hasegawa, P.M.; Bressan, R.A.; Zhu, J.-K.; Bohnert, H.J. Plant cellular and molecular responses to high salinity. *Annu. Rev. Plant Physiol. Plant Mol. Biol.* **2000**, *51*, 463–499. [[CrossRef](#)]
55. Zrig, A.; Mohamed, H.B.; Tounekti, T.; Ennajeh, M.; Valero, D.; Khemira, H. A comparative study of salt tolerance of three almond rootstocks: Contribution of organic and inorganic solutes to osmotic adjustment. *J. Agric. Sci. Technol.* **2015**, *17*, 675–689.
56. Munns, R.; Gilliam, M. Salinity tolerance of crops—what is the cost? *New Phytol.* **2015**, *208*, 668–673. [[CrossRef](#)]
57. Kozłowski, T.T.; Pallardy, S.G. Acclimation and adaptive responses of woody plants to environmental stresses. *Bot. Rev.* **2002**, *68*, 270–334. [[CrossRef](#)]
58. Munns, R.; Termaat, A. Whole-plant responses to salinity. *Funct. Plant Biol.* **1986**, *13*, 143. [[CrossRef](#)]
59. Nicotra, A.B.; Atkin, O.K.; Bonser, S.P.; Davidson, A.M.; Finnegan, E.J.; Mathesius, U.; Poot, P.; Purugganan, M.D.; Richards, C.L.; Valladares, F.; et al. Plant phenotypic plasticity in a changing climate. *Trends Plant Sci.* **2010**, *15*, 684–692. [[CrossRef](#)] [[PubMed](#)]
60. Maggio, A.; Raimondi, G.; Martino, A.; De Pascale, S. Salt stress response in tomato beyond the salinity tolerance threshold. *Environ. Exp. Bot.* **2007**, *59*, 276–282. [[CrossRef](#)]
61. Isayenkov, S.V.; Maathuis, F.J.M. Plant salinity stress: Many unanswered questions remain. *Front. Plant Sci.* **2019**, *10*, 80. [[CrossRef](#)] [[PubMed](#)]
62. Rius-Garcia, X.; Videgain-Marco, M.; Casanova-Gascón, J.; Acuña-Rello, L.; Martín-Ramos, P. Comparative evaluation of salt tolerance in four self-rooted hazelnut (*Corylus avellana* L. and *Corylus americana* Walter) cultivars. *Agronomy* **2025**, *15*, 148. [[CrossRef](#)]
63. Ranjbarfordoei, A.; Samson, R.; Van Damme, P. Chlorophyll fluorescence performance of sweet almond [*Prunus dulcis* (Miller) D. Webb] in response to salinity stress induced by NaCl. *Photosynthetica* **2006**, *44*, 513–522. [[CrossRef](#)]
64. Jimenez, S.; Dridi, J.; Gutierrez, D.; Moret, D.; Irigoyen, J.J.; Moreno, M.A.; Gogorcena, Y. Physiological, biochemical and molecular responses in four *Prunus* rootstocks submitted to drought stress. *Tree Physiol.* **2013**, *33*, 1061–1075. [[CrossRef](#)]
65. Acosta-Motos, J.; Ortuño, M.; Bernal-Vicente, A.; Diaz-Vivancos, P.; Sanchez-Blanco, M.; Hernandez, J. Plant responses to salt stress: Adaptive mechanisms. *Agronomy* **2017**, *7*, 18. [[CrossRef](#)]
66. Stefanov, M.A.; Rashkov, G.D.; Borisova, P.B.; Apostolova, E.L. Changes in photosystem II complex and physiological activities in pea and maize plants in response to salt stress. *Plants* **2024**, *13*, 1025. [[CrossRef](#)] [[PubMed](#)]
67. Mihaljevic, I.; Viljevac Vuletic, M.; Tomas, V.; Horvat, D.; Zdunic, Z.; Vukovic, D. PSII photochemistry responses to drought stress in autochthonous and modern sweet cherry cultivars. *Photosynthetica* **2021**, *59*, 517–528. [[CrossRef](#)]
68. Baker, N.R. Chlorophyll fluorescence: A probe of photosynthesis in vivo. *Annu. Rev. Plant Biol.* **2008**, *59*, 89–113. [[CrossRef](#)] [[PubMed](#)]
69. Kalaji, H.M.; Jajoo, A.; Oukarroum, A.; Brestic, M.; Zivcak, M.; Samborska, I.A.; Cetner, M.D.; Łukasik, I.; Goltsev, V.; Ladle, R.J. Chlorophyll a fluorescence as a tool to monitor physiological status of plants under abiotic stress conditions. *Acta Physiol. Plant* **2016**, *38*, 102. [[CrossRef](#)]
70. Negrão, S.; Schmöckel, S.M.; Tester, M. Evaluating physiological responses of plants to salinity stress. *Ann. Bot.* **2017**, *119*, 1–11. [[CrossRef](#)] [[PubMed](#)]
71. Chaves, M.M.; Flexas, J.; Pinheiro, C. Photosynthesis under drought and salt stress: Regulation mechanisms from whole plant to cell. *Ann. Bot.* **2009**, *103*, 551–560. [[CrossRef](#)] [[PubMed](#)]

72. Läuchli, A.; Grattan, S.R. Plant responses to saline and sodic conditions. In *Agricultural Salinity Assessment and Management*, 2nd ed.; Wallender, W.W., Tanji, K.K., Eds.; American Society of Civil Engineers: Reston, VA, USA, 2011; pp. 169–205. [[CrossRef](#)]
73. Hochberg, U.; Degu, A.; Fait, A.; Rachmilevitch, S. Near isohydric grapevine cultivar displays higher photosynthetic efficiency and photorespiration rates under drought stress as compared with near anisohydric grapevine cultivar. *Physiol. Plant.* **2012**, *147*, 443–452. [[CrossRef](#)] [[PubMed](#)]
74. Atar, F.; Güney, D.; Bayraktar, A.; Yildirim, N.; Turna, İ. Seasonal change of chlorophyll content (SPAD value) in some tree and shrub species. *Turk. J. For. Sci.* **2020**, *4*, 245–256. [[CrossRef](#)]
75. Stepien, P.; Johnson, G.N. Contrasting responses of photosynthesis to salt stress in the glycophyte *Arabidopsis* and the halophyte *Thellungiella*: Role of the plastid terminal oxidase as an alternative electron sink. *Plant Physiol.* **2009**, *149*, 1154–1165. [[CrossRef](#)]
76. Ashraf, M.; Harris, P.J.C. Photosynthesis under stressful environments: An overview. *Photosynthetica* **2013**, *51*, 163–190. [[CrossRef](#)]
77. Dejampour, J.; Aliasgarzad, N.; Zeinalabedini, M.; Niya, M.R.; Hervan, E.M. Evaluation of salt tolerance in almond [*Prunus dulcis* (L.) Batsch] rootstocks. *Afr. J. Biotechnol.* **2012**, *11*, 11907–11912. [[CrossRef](#)]
78. Rahnesan, Z.; Nasibi, F.; Moghadam, A.A. Effects of salinity stress on some growth, physiological, biochemical parameters and nutrients in two pistachio (*Pistacia vera* L.) rootstocks. *J. Plant Interact.* **2018**, *13*, 73–82. [[CrossRef](#)]
79. Momenpour, A.; Imani, A. Effect of salinity stress on growth characteristics of selected almond (*Prunus dulcis*) genotypes. *J. Plant Prod. Res.* **2019**, *26*, 29–46.
80. Tavakkoli, E.; Rengasamy, P.; McDonald, G.K. High concentrations of Na⁺ and Cl⁻ ions in soil solution have simultaneous detrimental effects on growth of faba bean under salinity stress. *J. Exp. Bot.* **2010**, *61*, 4449–4459. [[CrossRef](#)] [[PubMed](#)]
81. Flowers, T.J.; Colmer, T.D. Plant salt tolerance: Adaptations in halophytes. *Ann. Bot.* **2015**, *115*, 327–331. [[CrossRef](#)] [[PubMed](#)]
82. Rengel, Z. The role of calcium in salt toxicity. *Plant Cell Environ.* **1992**, *15*, 625–632. [[CrossRef](#)]
83. Läuchli, A.; Grattan, S.R. Plant growth and development under salinity stress. In *Advances in Molecular Breeding Toward Drought and Salt Tolerant Crops*; Jenks, M.A., Hasegawa, P.M., Jain, S.M., Eds.; Springer: Dordrecht, The Netherlands, 2007; pp. 1–32. [[CrossRef](#)]
84. Hasegawa, P.M. Sodium (Na⁺) homeostasis and salt tolerance of plants. *Environ. Exp. Bot.* **2013**, *92*, 19–31. [[CrossRef](#)]
85. Anshütz, U.; Becker, D.; Shabala, S. Going beyond nutrition: Regulation of potassium homeostasis as a common denominator of plant adaptive responses to environment. *J. Plant Physiol.* **2014**, *171*, 670–687. [[CrossRef](#)] [[PubMed](#)]
86. Shabala, S.; Pottosin, I. Regulation of potassium transport in plants under hostile conditions: Implications for abiotic and biotic stress tolerance. *Physiol. Plant.* **2014**, *151*, 257–279. [[CrossRef](#)]
87. Shabala, S.; Cuin, T.A. Potassium transport and plant salt tolerance. *Physiol. Plant.* **2008**, *133*, 651–669. [[CrossRef](#)]
88. Teakle, N.L.; Tyerman, S.D. Mechanisms of Cl⁻ transport contributing to salt tolerance. *Plant Cell Environ.* **2010**, *33*, 566–589. [[CrossRef](#)] [[PubMed](#)]
89. Papadakis, I.E.; Veneti, G.; Chatzissavvidis, C.; Therios, I. Physiological and growth responses of sour cherry (*Prunus cerasus* L.) plants subjected to short-term salinity stress. *Acta Bot. Croat.* **2018**, *77*, 197–202. [[CrossRef](#)]
90. Massai, R.; Remorini, D.; Tattini, M. Gas exchange, water relations and osmotic adjustment in two scion/rootstock combinations of *Prunus* under various salinity concentrations. *Plant Soil* **2004**, *259*, 153–162. [[CrossRef](#)]
91. Li, B.; Tester, M.; Gilliam, M. Chloride on the move. *Trends Plant Sci.* **2017**, *22*, 236–248. [[CrossRef](#)]
92. El Yamani, M.; Cordovilla, M.d.P. Tolerance mechanisms of olive tree (*Olea europaea*) under saline conditions. *Plants* **2024**, *13*, 2094. [[CrossRef](#)] [[PubMed](#)]
93. Malakar, P.; Chattopadhyay, D. Adaptation of plants to salt stress: The role of the ion transporters. *J. Plant Biochem. Biotechnol.* **2021**, *30*, 668–683. [[CrossRef](#)]
94. Mansour, M.M.F. Role of vacuolar membrane transport systems in plant salinity tolerance. *J. Plant Growth Regul.* **2022**, *42*, 1364–1401. [[CrossRef](#)]
95. Shabala, S. Learning from halophytes: Physiological basis and strategies to improve abiotic stress tolerance in crops. *Ann. Bot.* **2013**, *112*, 1209–1221. [[CrossRef](#)]
96. Reddy, A.A. The soil health card Scheme in India: Lessons learned and challenges for replication in other developing countries. *J. Nat. Resour. Policy. Res.* **2019**, *9*, 124–156. [[CrossRef](#)]

Disclaimer/Publisher’s Note: The statements, opinions and data contained in all publications are solely those of the individual author(s) and contributor(s) and not of MDPI and/or the editor(s). MDPI and/or the editor(s) disclaim responsibility for any injury to people or property resulting from any ideas, methods, instructions or products referred to in the content.